THE JOURNAL OF PHYSICAL CHEMISTRY A

ARTICLE

pubs.acs.org/JPCA

# Electronic Structure and Thermochemical Properties of Small Neutral and Cationic Lithium Clusters and Boron-Doped Lithium Clusters: $Li_n^{0/+}$ and $Li_nB^{0/+}$ ($n$ = 1−8)

Truong Ba Tai,[†] Pham Vu Nhat,[†] Minh Tho Nguyen,*[,†] Shenggang Li,[‡] and David A. Dixon*[,‡]

[†]Department of Chemistry, and Mathematical Modeling and Computational Science Center (LMCC), Katholieke Universiteit Leuven, B-3001 Leuven, Belgium

[‡]Department of Chemistry, The University of Alabama, Shelby Hall, Box 870336, Tuscaloosa, Alabama 35847-0336, United States

Supporting Information

**ABSTRACT:** The stability, electronic structure, and thermochemical properties of the pure $Li_n$ and boron-doped $Li_nB$ ($n$ = 1−8) clusters in both neutral and cationic states are studied using electronic structure methods. The global equilibrium structures are established, and their heats of formation are evaluated using the G3B3 and CCSD(T)/CBS methods based on the density functional theory geometries. Theoretical adiabatic ionization energies ($IE_a$) for the $Li_n$ clusters are in good agreement with experiment: $Li_2$ (G3B3, 5.21 eV; CCSD(T), 5.14 eV; expt, 5.1127 ± 0.0003 eV), $Li_3$ (4.16, 4.11, 4.08 ± 0.10), $Li_4$ (4.76, 4.68, 4.70 ± 0.05), $Li_5$ (4.11, 4.06, 4.02 ± 0.10), $Li_6$ (4.46, 4.32, 4.20 ± 0.10), $Li_7$ (4.07, 3.99, 3.94 ± 0.10), and $Li_8$ (4.49, 4.31, 4.16 ± 0.10). The $Li_4$ experimental $IE_a$ has been revised on the basis of the Franck−Condon simulations. Species $Li_5B$, $Li_6B^+$, $Li_7B$, and $Li_8B^+$ exhibit high stability as compared to their neighbors, which can be understood by considering the magic numbers of the phenomenological shell model (PSM).

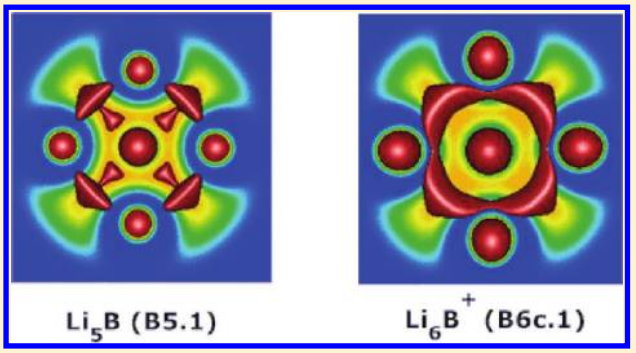


## INTRODUCTION

Lithium and lithium-based clusters continue to attract attention because of their interesting physical and chemical properties. A large number of studies on the spectroscopic parameters,[1−4] stabilities, and bonding nature[5−19] of the bare lithium clusters have been reported using various experimental and theoretical methods. It is well established that the addition of an impurity to a cluster can lead to fundamental changes in their geometries, energy properties, and bonding nature, leading to new materials. Because evidence of trilithium oxide $Li_3O$ was reported,[20] a number of studies of lithium-rich binary clusters have been carried out. Jiang et al.[21] and Deshpande et al.[22] reported on the structures and electronic properties of $Li_nX$ with X = K, Na. Baruah and Kanhere[23] reported a topological study of the charge densities of small clusters $Li_nX$ with X = Mg, Be and $n$ = 1−6. Theoretical investigations of $Li_nX$ with X = Mg, Be and $n$ = 1−12 were carried out by Deshpande et al.[24] using Car−Parrinello molecular dynamics (CPMD) simulations. Recently, studies of lithium-rich clusters with various impurities including aluminum,[25−33] carbon,[34−38] tin,[39−41] germanium,[42,43] and oxygen[10,44] have been reported. Mixed clusters containing boron and lithium have been investigated.[45−48] Lammertsma and co-workers[47] reported theoretical studies of $Li_nB$ ($n$ = 1−8) using various computational methods (B3LYP, MP2, G2MP2, SCF, and CASSCF). The structure and stability of $Li_nB$ ($n$ = 1−7) in both neutral and cationic states was predicted by Li et al.[46] using the coupled-cluster theory CCSD(T) method with the aug-cc-pVDZ basis set.

Despite numerous studies, discrepancies still exist in terms of the electronic structure and the global minima of some small clusters of $Li_n$[7,9,10,12,13,18] because of the different computational levels, for example, $Li_4$. Whereas most theoretical studies agree with each other that the planar structure ($D_{2h}$, $^1A_g$) is the global minimum of neutral $Li_4$,[9−11,14] the difference between the experimental and theoretical results with respect to the ionization energy (IE) is remarkably large. At the CCST(T)/cc-pwCVQZ level,[14] the IE value of $Li_4$ was reported to be 4.76 eV, which deviates substantially from the available experimental value of 4.31 eV. (More detail is provided below.) A complete interpretation of this difference remains a challenging issue. In addition, the electronic structures of boron-doped lithium clusters have not been studied in great detail yet, and their thermochemical properties have not been determined using reliable theoretical methods.

To expand our understanding of the properties of these clusters, we have performed a systematic series of calculations to predict the electronic structure, stabilities, and thermochemical properties of

**Received:** January 30, 2011
**Revised:** May 25, 2011
**Published:** June 14, 2011

bare $Li_n$ ($n$ = 1−8) and boron-doped $Li_nB$ ($n$ = 1−8) lithium clusters in both neutral and cationic states using high-accuracy computational methods. The electronic structure and thermochemical properties of bare lithium clusters $Li_n^{0/+}$ are re-examined by using high-level G3B3 and CCSD(T)/complete basis set (CBS) methods. The electronic structure, stability, chemical bonding, and thermochemical properties of boron-doped lithium clusters $Li_nB$ in both cationic and neutral states are investigated in detail. The global minima of $Li_n$ are established and compared to previous reports, and the experimental spectrum of $Li_4$ is reassigned on the basis of a comparison of the experimental spectra and our simulated photoionization spectra. New global minima are found including those of $Li_2B^{0/+}$, $Li_3B^+$, $Li_4B$, and $Li_8^{0/+}$. The growth mechanism of $Li_nB$ clusters can then be analyzed with this data. The stability of these molecules is also considered in terms of their chemical properties. In particular, the enhanced stability of the $Li_5B$, $Li_6B^+$, $Li_7B$, and $Li_8B^+$ species can be rationalized by using the phenomenological shell model (PSM).[49]

## COMPUTATIONAL METHODS

All electronic structure calculations are carried out by using the Gaussian 03[50] and Molpro 2008.1[51] program packages. Equilibrium geometries and harmonic vibrational frequencies of the $Li_n$ and $Li_nB$ ($n$ = 1−8) clusters in both neutral and cationic states are calculated at the density functional theory (DFT) level with the hybrid B3LYP functional[52−54] in conjunction with the correlation-consistent aug-cc-pVTZ basis set for Li and B.[55] To obtain improved results, the geometries, energies, and frequencies of the lowest isomers of all clusters ($n$ = 1−8) were optimized at the CCSD(T) (R/UCCSD(T) for open-shell species) level[56] with the aV$n$Z basis sets ($n$ = D, T) and the G3B3 approach.[57] The aV$n$Z basis set is a combination of the cc-pVXZ basis set for Li[58] and the aug-cc-pVXZ basis set for B. For the lowest-energy structures, the coupled-cluster calculations were also carried out with the aVQZ basis set with the energies extrapolated to the complete basis set (CBS) limit using a mixed exponential/Gaussian expression.[59] Because we are extrapolating to the CBS limit, there is no basis set superposition error. In the above CCSD(T) calculations, the $1s^2$ electrons on Li and B are excluded from the correlation treatment. Core−valence correlation corrections to the CCSD(T) energies for the $1s^2$ electrons on Li and B are calculated at the CCSD(T)/aug-cc-pwCVTZ level (cc-pwCVTZ for Li).[60] The scalar relativistic corrections were calculated with the second-order Douglas−Kroll−Hess Hamiltonian[61] as the difference between the valence electron energies at the CCSD(T)-DK/aug-cc-pwCVTZ-DK and CCSD(T)/aug-cc-pwCVTZ levels (without the augmented functions for Li).[62,63] The procedures for evaluating these energies are given in detail in our recent papers[64−66] on other boron compounds. Total atomization energies (TAEs) are subsequently calculated using the composite G3B3 and CCSD(T)/CBS approaches. By combining the calculated TAE values with the known heats of formation at 0 K for the elements, $\Delta_fH$(B) = 135.1 ± 0.2 kcal/mol[67] and $\Delta_fH$ (Li) = 37.7 ± 0.2 kcal/mol,[68] the $\Delta_fH$ values at 0 K of the $Li_n$ and $Li_nB$ clusters can be calculated. A rationale for the choice of the heat of formation for B and Li has been given.[69] The heats of formation at 298 K are then calculated from the thermal corrections.[70] To assess previous assignments of the photoionization efficiency spectra for a better comparison between calculated and experimental adiabatic ionization potentials for $Li_n$, the photoelectron spectrum for the transition from the ground state of the neutral cluster to that of the cation was simulated[71] and was integrated to yield the photoionization efficiency spectrum.

The structures are analyzed in terms of natural bond orbitals (NBO)[72−74] constructed using the B3LYP/6-311+G(d) densities. To understand better the nature of the chemical bonding phenomenon, an analysis of the electron localization function (ELF)[75] supplemented by a determination of their topological bifurcations[76] is performed. The ELF is a local measure of electron repulsion in 3D space due to the Pauli exclusion principle. Such a localization technique allows the partitioning of the total density into basins, which correspond to molecular regions containing the cores, lone pairs, and chemical bonds. The total ELFs are mapped out using TOPMOD software,[77] and all ELF isosurfaces are plotted using Gopenmol software.[78]

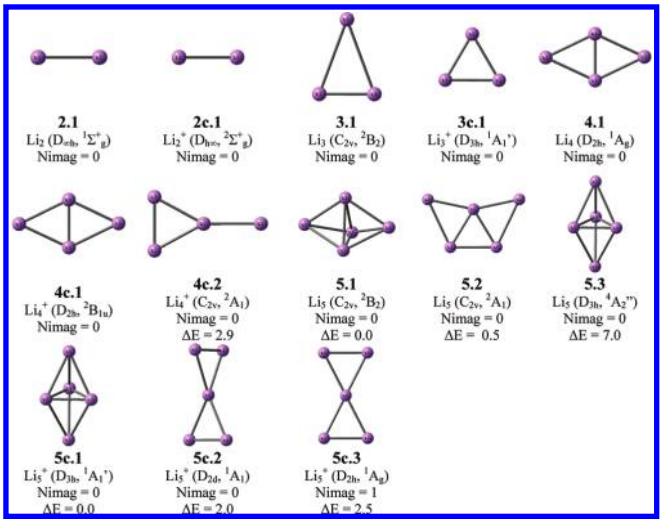


**Figure 1.** Optimized structures for $Li_n$ and $Li_n^+$ ($n$ = 2−6) and relative energies at 0 K ($\Delta E$, kcal/mol) calculated at the B3LYP/aug-cc-pVTZ level.

## RESULTS

**Structures of $Li_n$ and $Li^{n+}$ and Ionization Energies of $Li_n$.** A variety of $Li_n$ structures were constructed starting from isomers reported in previous studies, and additional new isomers were also studied. All structures are fully optimized and characterized at the B3LYP/aug-cc-pVTZ level. The optimized geometries of a selection of lower-lying $Li_n$ clusters in both neutral and cationic states, together with their relative energies (kcal/mol), are shown in Figures 1 and 2. The Cartesian coordinates of the B3LYP/aug-cc-pVTZ-optimized geometries of all isomers considered are listed in the Supporting Information. The energy properties of the lowest-energy isomers of $Li_n$ are predicted by using the higher-level G3B3 and CCSD(T)/CBS methods. The heats of formation derived using the total atomization energies, $\Sigma D_0$, obtained from the G3B3 and CCSD(T)/CBS methods are given in Table 1. The limited available experimental data for these quantities are given. The calculated adiabatic ionization energies ($IE_a$) at the above levels are compiled in Table 2 and compared with available experimental data for $Li_n$.[79] The ground states of the $Li_n$ clusters and their cations have no significant multireference character as indicated by the relatively small $T_1$ diagnostics[80] of <0.02 except for $Li_6^+$ and $Li_8^+$, where the $T_1$

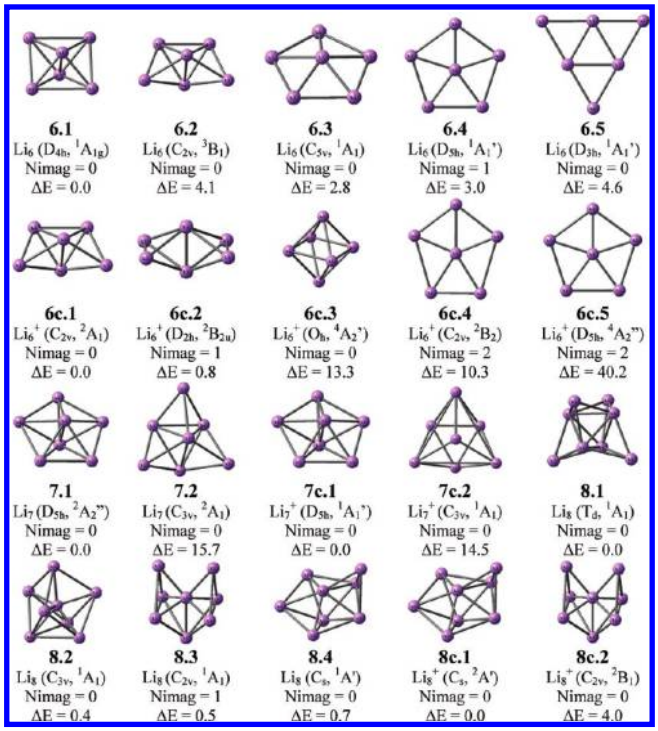


**Figure 2.** Optimized structures for $Li_n$ and $Li_n^+$ ($n$ = 7−8) and relative energies at 0 K ($\Delta E$, kcal/mol) calculated at the B3LYP/aug-cc-pVTZ level.

diagnostics are slightly larger at 0.032 and 0.024 (Supporting Information). The structures given hereafter are labeled **n.x** for the neutral and **nc.x** for the cations, where **n** stands for the size and **c** stands for the cation. For the sake of a systematic comparison, only the relative energies derived from the B3LYP calculations are given in the Figures.

**$Li_2$ and $Li_2^+$.** The smallest clusters $Li_n$ ($n$ = 2−4) have been extensively studied, and our G3B3 and CCSD(T)/CBS results agree well with earlier calculations. The ground states of $Li_2$ and $Li_2^+$ are $^1\Sigma^+_g$ and $^2\Sigma^+_g$, respectively. The calculated Li−Li distances of $Li_2$ are 2.698 and 2.670 Å at the B3LYP/aug-cc-pVTZ and CCSD(T)/cc-pVQZ levels, respectively, in good agreement with the experimental value of 2.672 Å.[81] Our calculated values are comparable to the values calculated at the CCSD(T)/cc-pwCVTZ (2.677 Å) and CCSD(T)/cc-pwCVQZ (2.674 Å) levels,[14a] where the $1s^2$ electrons on Li were also correlated. The calculated heat of formation at 298 K of 51.7 kcal/mol for $Li_2$ at the CCSD(T)/CBS level is in excellent agreement with the experimental value of 51.6 ± 0.7 kcal/mol.[68]

Our calculated Li−Li distance of 3.132 Å at the CCSD(T)/cc-pVQZ level for the cation compares well with the experimental value of 3.12 Å,[82] which is also close to the value of 3.099 Å obtained at the CCSD(T)/cc-pwCVQZ level.[14b] The calculated adiabatic ionization energies of $Li_2$ are 5.21 (G3B3) and 5.14 eV (CCSD(T)/CBS); the latter is in very good agreement with the experimental value of 5.1127 ± 0.0003 eV.[83] Our calculated ionization energies are essentially the same as that calculated by Wheeler and Schaefer[14b] of 5.14 eV at the CCSD(T)/cc-pwCVQZ level.

**$Li_3$ and $Li_3^+$.** Low-spin neutral structure **3.1** ($C_{2v}$, $^2B_2$), distorted from $D_{3h}$ symmetry because of the Jahn−Teller effect, is predicted to be the global minimum for $Li_3$, consistent with previous studies.[9−11,14] At the CCSD(T)/cc-pVQZ level, the bond angle of 71.8° found for **3.1** agrees well with a previous theoretical prediction of 71.8° at the CCSD(T)/cc-pwCVQZ level.[14a] There is a $^2A_1$ state with an acute angle of 54.1° that is 1.2 kcal/mol higher in energy and has one imaginary frequency of 159i $cm^{-1}$. The Li−Li bond lengths in the $^2B_2$ state of $Li_3$ calculated by CCSD(T)/cc-pVQZ are 2.789 (×2) and 3.272 Å, whereas the B3LYP values are 2.631 (×2) and 3.048 Å; the experimental values are 2.73 and 3.20 Å.[4]

High-symmetry structure **3c.1** ($D_{3h}$, $^1A_1'$) is the global minimum for $Li_3^+$ (Figure 1). The calculated values for the $IE_a$ of $Li_3$ are 4.16 eV (G3B3) and 4.11 eV (CCSD(T)/CBS), which can be compared to the calculated value of 4.11 eV at the CCSD(T)/cc-pwCVQZ level[14b] and the experimental value of 4.08 ± 0.10 eV.[79]

**$Li_4$ and $Li_4^+$.** In agreement with previous reports,[9−11,14] planar structure **4.1** ($D_{2h}$, $^1A_g$) is predicted to be the global minimum for $Li_4$. However, the $^1A_1$ state of the $C_{2v}$ structure of $Li_4$ (not shown) was predicted to have an imaginary frequency of ~70i $cm^{-1}$ at the B3LYP, MP2, and CCSD(T) levels, and it lies higher in energy than the $^1A_g$ state of the $D_{2h}$ structure by 7 to 11 kcal/mol. Optimizing this $C_{2v}$ structure by following the eigenvector of the imaginary frequency leads to the $D_{2h}$ structure. Thus, the $^1A_1$ state of the $C_{2v}$ structure is a transition state connecting the different $^1A_g$ states of the $D_{2h}$ structures resulting from capping the $Li_3$ triangular structure on its different sides.

**Table 1. Calculated Heats of Formation ($\Delta_f H$, kcal/mol) for the Lowest-Energy Isomers of $Li_n^{0/+}$ at 0 and 298 K at the G3B3 and CCSD(T)/CBS Levels[a,b]**

| | | $\Delta_f H$ (0 K) | | $\Delta_f H$ (298 K) | |
|---|---|---|---|---|---|
| molecule | label | G3B3 | CCSD(T) | G3B3 | CCSD(T) |
| $Li_2$ ($^1\Sigma^+_g$) | **2.1** | 49.1 | 51.6 | 49.2 | 51.7 |
| $Li_3$ ($^2B_2$) | **3.1** | 72.9 | 75.9 | 72.6 | 76.0 |
| $Li_4$ ($^1A_g$) | **4.1** | 78.8 | 83.8 | 78.9 | 83.8 |
| $Li_5$ ($^2B_2$) | **5.1** | 95.2 | 100.9 | 95.3 | 100.7 |
| $Li_5$ ($^2A_1$) | **5.2** | 97.6 | | 97.8 | |
| $Li_6$ ($^1A_{1g}$) | **6.1** | 98.1 | 106.9 | 98.1 | 106.8 |
| $Li_6$ ($^1A_1$) | **6.3** | 103.6 | | 103.9 | |
| $Li_7$ ($^2A_2''$) | **7.1** | 105.2 | 115.1 | 105.1 | 114.9 |
| $Li_7$ ($^2A_1$) | **7.2** | 110.8 | | 110.8 | |
| $Li_8$ ($^1A_1$) | **8.1** | 112.4 | 123.6 | 112.4 | 123.5 |
| $Li_8$ ($^1A_1$) | **8.2** | 112.0 | | 112.1 | |
| $Li_2^+$ ($^2\Sigma^+_g$) | **2c.1** | 169.4 | 170.1 | 169.6 | 170.3 |
| $Li_3^+$ ($^1A_1'$) | **3c.1** | 168.9 | 170.6 | 168.9 | 170.6 |
| $Li_4^+$ ($^2B_{1u}$) | **4c.1** | 188.7 | 191.6 | 188.9 | 191.8 |
| $Li_4^+$ ($^2A_1$) | **4c.2** | 190.5 | | 190.8 | |
| $Li_5^+$ ($^1A_1'$) | **5c.1** | 190.0 | 194.4 | 190.0 | 194.3 |
| $Li_5^+$ ($^1A_1$) | **5c.2** | 194.6 | | 195.0 | |
| $Li_6^+$ ($^2A_1$) | **6c.1** | 200.9 | 206.6 | 200.9 | 206.6 |
| $Li_6^+$ ($^2B_{2u}$) | **6c.3** | 201.1 | | 200.6 | |
| $Li_7^+$ ($^1A_1'$) | **7c.1** | 199.1 | 207.0 | 199.0 | 206.9 |
| $Li_7^+$ ($^1A_1$) | **7c.2** | 204.7 | | 204.8 | |
| $Li_8^+$ ($^2A'$) | **8c.1** | 215.9 | 223.0 | 216.0 | 223.1 |
| $Li_8^+$ ($^2B_1$) | **8c.2** | 219.9 | | 220.1 | |

[a] Includes core−valence and scalar relativistic corrections and zero-point energies. [b] The ion heats of formation at 298 K were calculated in the ion convention where the electron has 0 kcal/mol for the integrated heat capacity of the electron.


dx.doi.org/10.1021/jp200992u | J. Phys. Chem. A 2011, 115, 7673–7686

**Table 2. Calculated Adiabatic Ionization Energies (eV) of the $Li_n$ Clusters ($n$ = 1−8) Using the CCSD(T)/CBS and G3B3 Methods Compared with Experiment**

| neutral | cation | G3B3 | CCSD(T)/cc-pVTZ | CCSD(T)/CBS[a] | expt[b] |
|---|---|---|---|---|---|
| Li ($^2S_{1/2}$) | $Li^+$ ($^1S_0$) | 5.40 | 5.38[c] | 5.39[c] | 5.391719[d] |
| $Li_2$ ($D_{\infty h}$, $^1\Sigma^+_g$) | $Li_2^+$ ($D_{\infty h}$, $^2\Sigma^+_g$) | 5.21 | 5.09 | 5.14 | 5.1127 ± 0.0003[e] |
| $Li_3$ ($C_{2v}$, $^2B_2$) | $Li_3^+$ ($D_{3h}$, $^1A_1'$) | 4.16 | 4.08 | 4.11 | 4.08 ± 0.1 |
| $Li_4$ ($D_{2h}$, $^1A_g$) | $Li_4^+$ ($D_{2h}$, $^2B_{1u}$) | 4.76 | 4.64 | 4.68 | 4.70 ± 0.05[f] |
| $Li_5$ ($C_{2v}$, $^2B_2$) | $Li_5^+$ ($D_{3h}$, $^1A_1'$) | 4.11 | 4.02 | 4.06 | 4.02 ± 0.1 |
| $Li_6$ ($D_{4h}$, $^1A_{1\,g}$) | $Li_6^+$ ($C_{2v}$, $^2A_1$) | 4.46 | 4.28 | 4.32 | 4.20 ± 0.1 |
| $Li_7$ ($D_{5h}$, $^2A_2''$) | $Li_7^+$ ($D_{5h}$, $^1A_1'$) | 4.07 | 3.96 | 3.99 | 3.94 ± 0.1 |
| $Li_8$ ($T_d$, $^1A_1$) | $Li_8^+$ ($C_s$, $^2A'$) | 4.49 | 4.25 | 4.31 | 4.16 ± 0.1 |

[a] Includes core−valence and scalar relativistic corrections. [b] Reference 79. [c] At the CCSD(T)/cc-pwCVXZ (X = D, T, Q) levels with Li $1s^2$ electrons correlated. [d] Reference 84. [e] Reference 83. [f] Reassigned experimental value based on our spectral simulations. See the text.

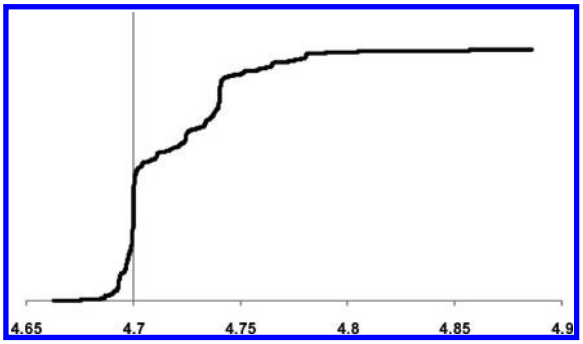


**Figure 3.** Simulated photoionization efficiency spectrum of $Li_4$ at 100 K at the B3LYP/cc-pVDZ level. The adiabatic ionization potential is set to 4.70 eV.

At the B3LYP level, structure **4c.1** ($D_{2h}$, $^2B_{1u}$) is found to be the lowest-energy isomer of $Li_4^+$, lower than isomer **4c.2** ($C_{2v}$, $^2A_1$) by ∼3 kcal/mol. However, at the CCSD(T) level, the $^2B_{1u}$ state was predicted to have one imaginary frequency of ∼130i $cm^{-1}$, whereas the $^2A_1$ state was predicted to be a minimum with no imaginary frequency. At the CCSD(T)/CBS level, the $^2B_{1u}$ state was predicted to be lower in energy than the $^2A_1$ state by ∼1.5 kcal/mol. The imaginary frequency calculated at the CCSD(T) level for the $^2B_{1u}$ state is likely due to symmetry breaking, as pointed out in a previous study.[14b] In addition, at the B3LYP/aug-cc-pVTZ and MP2/aug-cc-pVTZ levels, the $^2B_{1u}$ state was predicted to be a minimum with no imaginary frequency.

On the basis of the above results, either the $^2B_{1u} \leftarrow {}^1A_g$ transition or the $^2A_1 \leftarrow {}^1A_g$ transition should be used to explain the experimental photoionization efficiency spectrum.[79] However, the $^2A_1 \leftarrow {}^1A_g$ transition can be further ruled out because of the substantial change in the equilibrium geometries accompanying the ionization process. In fact, the experimental spectrum has a very sharp onset.[79] Thus, it can be assigned only to the $^2B_{1u} \leftarrow {}^1A_g$ transition, where there is little change in the equilibrium geometries. The simulated photoionization efficiency spectrum by integrating the intensity for the simulated photoelectron spectrum with the energy of the 0−0 band set to 4.70 eV is shown in Figure 3, which agrees fairly well with the experimental spectrum.[79] The weak signal observed at energies below 4.70 eV, which was used previously to assign the experimental $IE_a$ to 4.31 eV,[79] can be accounted for by the hot transitions from the vibrationally excited levels of the neutral ground state to the ground vibrational level of the cationic ground state, as also shown in Figure 3. On the basis of the above argument, the experimental $IE_a$ of $Li_4$ is readjusted to 4.70 ± 0.05 eV, which is now in excellent agreement with our calculated value of 4.68 eV at the CCSD(T)/CBS level. The G3B3 method gives a slightly overestimated value of 4.76 eV. Our CCSD(T)/CBS value for the $IE_a$ of $Li_4$ is also in good agreement the CCSD(T)/cc-pwCVQZ value of 4.74 eV.[14b] Thus, the experimental $IE_a$ of $Li_4$ had been misassigned because of the extrapolation of the tail resulting from the hot transitions.

**$Li_5$ and $Li_5^+$.** The pentaatomic clusters in both neutral and cationic states have been extensively investigated in previous studies using various methods. Boustani et al.[9] predicted the planar $Li_5$ **5.2** ($C_{2v}$, $^2A_1$) structure to be the most stable. In contrast, Jones et al.[10] predicted trigonal bipyramidal (TBP) structure **5.1** ($C_{2v}$) to be the global minimum. In a more recent study, Alexandrova et al.[7] also predicted that the global minimum of $Li_5$ is TBP structure **5.1** ($C_{2v}$, $^2B_1$) at the CCSD(T)/6-311+G(d) level. We explored a number of structures for $Li_5$ using both the G3B3 and CCSD(T) methods, and some of the lower-energy isomers are displayed in Figure 1. Our results confirm that TBP structure **5.1** ($C_{2v}$, $^2B_2$), which is Jahn−Teller distorted from $D_{3h}$, is the lowest-energy structure. However, planar structure **5.2** ($C_{2v}$, $^2A_1$) is only 2.4 kcal/mol (G3B3 value) less stable than **5.1**. High-spin structure **5.3** ($D_{3h}$, $^4A_2''$) is 7.0 kcal/mol less stable than **5.1**.

Removing one electron from the ground state of $Li_5$ also removes the first-order Jahn−Teller distortion. Thus, the ground state of $Li_5^+$ is **5c.1** ($D_{3h}$, $^1A_1'$) with higher symmetry than the neutral, just as in the case of $Li_3$ and $Li_3^+$. The next lowest energy isomer is **5c.2** ($D_{2d}$, $^1A_1$), which is only 2.0 kcal/mol higher in energy, in agreement with earlier results.[7] The $IE_a$ of $Li_5$ is calculated to be 4.06 (CCSD(T)/CBS) and 4.11 eV (G3B3), in good agreement with the experimental value of 4.02 ± 0.10 eV.[79]

**$Li_6$ and $Li_6^+$.** A number of computational studies have been carried out to identify the global minimum for $Li_6$. Boustani et al.[9] found two local energy minima (Figure 2), quasi-planar structure **6.3** ($C_{5v}$, $^1A_1$), and planar structure **6.5** ($D_{3h}$, $^1A_1'$) with the same energies at the CISD level. In contrast, Gardet et al.[12] predicted that 3D structure **6.2** is the most stable isomer. On the basis of DFT molecular dynamics simulations, Jones et al.[10] predicted that the global minimum of $Li_6$ is distorted octahedron **6.1** with $D_{4h}$ symmetry. The latter prediction was recently supported by Alexandrova and Boldyrev[7] in which **6.1** ($^1A_{1g}$) is at least 4.2 kcal/mol lower in energy than the other isomers at the CCSD(T)/6-311+G(d) level. Temelso and Sherrill[15] also identified structure **6.1** as the global minimum at the CCSD(T) level

with up to the quadruple ζ basis set including core−valence corrections, and they found good agreement between the experimental and simulated optical absorption spectra for this structure. Our calculations also predict structure **6.1** to be the global minimum. Structure **6.3** ($C_{5v}$, $^1A_1$), which is distorted from structure **6.4** with higher symmetry ($D_{5h}$), is found to be the second most stable isomer with a relative energy of 2.8 kcal/mol above that of **6.1** at the B3LYP/aug-cc-pVTZ level. Planar structure **6.5** ($D_{3h}$, $^1A_1'$) is the next higher energy structure and is 4.6 kcal/mol less stable than **6.1** at the B3LYP/aug-cc-pVTZ level.

Because the HOMO of structure **6.1** is a doubly degenerate orbital of $e_u$ symmetry, removing one electron from its HOMO will result in a Jahn−Teller distorted cationic structure with a lower symmetry than $D_{4h}$. The $^2B_{2u}$ state of the $D_{2h}$ structure (**6c.2**) was initially predicted[9] to be the global minimum of $Li_6^+$. Temelso and Sherrill[15] predicted $Li_6^+$ to have $C_{2v}$ symmetry (**6c.1**) upon distortion from $D_{4h}$. However, the $^2B_2$ state of $C_{2v}$ symmetry (**6c.4**) resulting from distorting the $C_{5v}$ structure (**6.3**) was predicted to be the global minimum by Alexandrova and Boldyrev.[7] Our calculated results are consistent with those by Temelso and Sherrill.[15] The $e_u$ orbitals under $D_{4h}$ correspond to the $a_1$ and $b_2$ orbitals under $C_{2v}$, which is a subgroup of $D_{4h}$ symmetry. Removing an electron from the $a_1$ orbital results in the $^2A_1$ state of $C_{2v}$ symmetry (**6c.1**) after geometry optimization. Removing an electron from the $b_2$ orbital results in the $^2B_{2u}$ state of $D_{2h}$ symmetry (**6c.2**) after geometry optimization. The $^2B_{2u}$ state (**6c.2**) is only 0.8, 0.2, and 0.6 kcal/mol higher in energy than the $^2A_1$ state (**6c.1**) at the B3LYP, CCSD(T), and G3B3 levels, and the $^2B_{2u}$ state is a transition state with an imaginary frequency of 62 $cm^{-1}$ connecting the $^2A_1$ states (**6c.1**) resulting from the elongations of different pairs of neighboring Li atoms in the equatorial positions. Thus, the energy barrier for going from one Jahn−Teller distorted structure to another for structure **6c.1** is very small (i.e., structure **6c.1** is very fluxional). In addition, the other isomer for the cation is higher in energy than **6c.1** by >13 kcal/mol.

The $IE_a$ for $Li_6$ was predicted to be 4.32 eV at the CCSD(T)/CBS level, which agrees well with the experimental value of 4.20 ± 0.10 eV[79] and that of 4.27 eV by Temelso and Sherrill[15] at the CCSD(T)/cc-pCVDZ level. Although the equilibrium geometries for the ground states of $Li_6$ and $Li_6^+$ (**6.1** and **6c.1**) are substantially different, the experimental photoionization spectrum has a fairly sharp onset, which is likely due to the fluxional nature of the cationic structure.

**$Li_7$ and $Li_7^+$.** The global minima for $Li_7$ and $Li_7^+$ located in the present work are in good agreement with previous studies.[7,9,10] Our calculations predict structure **7.1** ($D_{5h}$, $^2A_2''$) to be the most stable isomer for $Li_7$, with structure **7.2** ($C_{3v}$, $^2A_1$) being the second lowest energy isomer (Figure 2).

Removing one electron from **7.1** results in structure **7c.1** ($D_{5h}$, $^1A_1'$) of the cation, which has similar geometry to that of the neutral cluster. Structure **7c.1** was predicted to be the global minimum for $Li_7^+$. Structure **7c.2** ($C_{3v}$, $^1A_1$) is 14.5 kcal/mol higher in energy than structure **7c.1**.[9] Our calculated $IE_a$ for $Li_7$ at the CCSD(T)/CBS level of 3.99 eV is in good agreement with the experimental value of 3.94 ± 0.10 eV.[79] Our G3B3 value of 4.07 eV for its $IE_a$ is slightly larger and just outside of the error bars.

**$Li_8$ and $Li_8^+$.** Various structures have been assigned to the global minimum of $Li_8$. Reichardt et al.[18] suggested $C_{3v}$ structure **8.2** to be the global minimum. Fourier et al.[13] located similar structure **8.3** for $Li_8$ but with the lower symmetry of $C_{2v}$. Using different approaches, Boustani et al.,[9] Gardet et al.,[12] and Jones et al.[10] predicted high-symmetry $T_d$ structure **8.1** to be the most stable isomer of $Li_8$. According to our G3B3 and CCSD(T)/cc-pVTZ calculations, there is a negligible energy difference between these local minima (Figure 2). Structure **8.2** ($C_{3v}$, $^1A_1$) is more stable by 0.4 kcal/mol than structure **8.1** ($T_d$, $^1A_1$) at the G3B3 level, whereas at the CCSD(T)/cc-pVTZ level, structure **8.1** ($T_d$, $^1A_1$) is 0.1 kcal/mol more stable than structure **8.2**. Structure **8.3** ($C_{2v}$, $^1A_1$) is a transition state connecting the **8.2** structures. Isomer **8.4** ($C_s$, $^1A'$), in which one lithium atom is absorbed on one of the triangular faces of structure **7.1** ($D_{5h}$), is only 0.7 kcal/mol less stable than structure **8.1**.

The removal of one electron from the doubly degenerate HOMO of structure **8.1** of $Li_8$ leads to a Jahn−Teller distorted structure with $C_s$ symmetry. Structure **8c.1** ($C_s$, $^2A'$) is more stable than isomer **8c.2** ($C_{2v}$, $^2B_1$) by 4.0 kcal/mol at the B3LYP/aug-cc-pVTZ level (Figure 2). The calculated $IE_a$ of $Li_8$ of 4.31 eV (CCSD(T)/CBS) is consistent with the experimental value of 4.16 ± 0.10 eV.[79]

**Structures of $Li_nB$ and $Li^nB^+$ and Ionization Energies of $Li_nB$.** The initial structures for $Li^nB$ are constructed either from the structures reported previously[45−47] or by replacing one Li atom of $Li_{n+1}$ with one B atom at various positions or adding one B atom to the $Li_n$ cluster. All structures are initially optimized at the B3LYP/aug-cc-pVTZ level. The B3LYP geometries were then used as the starting geometries for the G3B3 and CCSD(T)/CBS calculations. The heats of formation for all global minima of $Li_nB$ and $Li_nB^+$ are calculated from the total atomization energies using the G3B3 and CCSD(T)/CBS approaches and are summarized in Table 4. The ground states of the $Li_nB$ clusters and their cations have no significant multireference characters as indicated by the relatively small $T_1$ diagnostics of <0.02 except in a few cases: $Li_3B$ (0.026), $Li_4B$ (0.041), $Li_5B$ (0.033), and $Li_3B$ (0.030) (Supporting Information). The difference between the CCSD(T)/CBS and G3B3 values generally increases as the size of the cluster increases and is ∼11 kcal/mol for $Li_8B$ and $Li_8B^+$, which reflects the degree of accuracy of the G3B3 results. As a convention, the structures are referred to hereafter as **Bn.x** and **Bnc.x**, where **B** stands for the dopant, **n** stands for the number of Li atoms, and **c** stands for the cation. In contrast to the pure $Li_n$ clusters, there is no experimental data available for these doped systems.

**LiB and $LiB^+$.** In agreement with previous reports,[45,47] the high-spin **B1** ($^3\Pi$) state is the ground state for LiB with an electron configuration of $(1\sigma^+)^2(2\sigma^+)^2(3\sigma^+)^2(4\sigma^+)^1(1\pi)^1$. At the CCSD(T)/CBS level, the $^1\Sigma^+$ state with an electron configuration of $(1\sigma^+)^2(2\sigma^+)^2(3\sigma^+)^2(4\sigma^+)^2$ and the $^3\Sigma^+$ state with an electron configuration of $(1\sigma^+)^2(2\sigma^+)^2(3\sigma^+)^2(1\pi)^2$ for LiB are predicted to be higher in energy by 6.0 and 10.7 kcal/mol, respectively, at 0 K. At the CCSD(T)/aVQZ level, the Li−B bond length and stretching frequency for LiB ($^3\Pi$) are 2.146 Å and 543 $cm^{-1}$, respectively, comparable to the values of 2.141 Å and 548 $cm^{-1}$ calculated at the QCISD/6-311+G(d) level.[47]

Low-spin **B1c** ($^2\Sigma^+$) is the ground state[45,47] for $LiB^+$ with an electron configuration of $(1\sigma^+)^2(2\sigma^+)^2(3\sigma^+)^2(4\sigma^+)^1$. The $^2\Pi$ state of $LiB^+$ with an electron configuration of $(1\sigma^+)^2(2\sigma^+)^2(3\sigma^+)^2(1\pi)^1$ is predicted to be higher in energy than the $^2\Sigma^+$ state by 15.6 kcal/mol at the CCSD(T)/CBS level at 0 K. At the CCSD(T)/aVQZ level, the Li−B bond length for $LiB^+$ ($^2\Sigma^+$) is ∼0.3 Å longer than that for LiB ($^3\Pi$), and the Li−B stretching frequency for $LiB^+$ ($^2\Sigma^+$) is ∼200 $cm^{-1}$ less. Natural population analysis shows a high ionic character for the Li−B bond in LiB

**Table 3. Dissociation Enthalpies ($\Delta H$, kcal/mol) of Lithium Clusters $Li_n$ and $Li^{n+}$ into Different Products[a]**

| molecule | products | $\Delta H$(0 K) G3B3 | $\Delta H$(298 K) G3B3 | $\Delta H$(0 K) CCSD(T)/CBS | $\Delta H$(298 K) CCSD(T)/CBS |
|---|---|---|---|---|---|
| $Li_2$ | 2Li | 26.3 | 27.0 | 23.8 | 24.5 |
| $Li_2^+$ | $Li + Li^+$ | 30.5 | 30.7 | 29.6 | 30.3 |
| $Li_3$ | $Li + Li_2$ | 13.9 | 14.7 | 13.4 | 13.8 |
| | 3Li | 40.2 | 41.7 | 37.2 | 38.3 |
| $Li_3^+$ | $Li + Li_2^+$ | 38.2 | 38.4 | 37.1 | 37.6 |
| | $Li_2 + Li^+$ | 42.4 | 42.9 | 42.8 | 43.3 |
| $Li_4$ | $Li + Li_3$ | 31.8 | 31.8 | 29.8 | 30.3 |
| | $2Li_2$ | 19.4 | 19.5 | 19.3 | 19.5 |
| | 4Li | 72.0 | 73.5 | 67.0 | 68.6 |
| $Li_4^+$ | $Li + Li_3^+$ | 17.9 | 17.7 | 16.7 | 17.3 |
| | $Li_2 + Li_2^+$ | 29.8 | 29.9 | 30.0 | 30.4 |
| | $Li_3 + Li^+$ | 46.4 | 46.3 | 46.2 | 46.9 |
| $Li_5$ | $Li + Li_4$ | 21.3 | 21.7 | 20.6 | 21.1 |
| | $Li_2 + Li_3$ | 26.8 | 26.5 | 26.5 | 26.8 |
| | 5Li | 93.3 | 95.2 | 87.6 | 89.7 |
| $Li_5^+$ | $Li + Li_4^+$ | 36.4 | 36.6 | 35.0 | 35.3 |
| | $Li_2 + Li_3^+$ | 28.0 | 28.1 | 27.8 | 28.0 |
| | $Li_3 + Li_2^+$ | 52.3 | 52.2 | 51.6 | 51.9 |
| | $Li_4 + Li^+$ | 51.0 | 51.5 | 51.3 | 51.8 |
| $Li_6$ | $Li + Li_5$ | 34.8 | 35.3 | 31.7 | 32.2 |
| | $Li_2 + Li_4$ | 29.8 | 30.0 | 28.4 | 28.6 |
| | $2Li_3$ | 47.7 | 47.1 | 44.9 | 44.3 |
| | 6Li | 128.1 | 130.5 | 119.3 | 121.7 |
| $Li_6^+$ | $Li + Li_5^+$ | 26.8 | 26.8 | 25.5 | 25.5 |
| | $Li_2 + Li_4^+$ | 36.9 | 37.2 | 36.6 | 36.9 |
| | $Li_3 + Li_3^+$ | 40.9 | 40.6 | 40.0 | 39.7 |
| | $Li_4 + Li_2^+$ | 47.3 | 47.6 | 47.3 | 47.6 |
| | $Li_5 + Li^+$ | 56.5 | 57.0 | 56.2 | 56.7 |
| $Li_7$ | $Li + Li_6$ | 30.6 | 31.1 | 29.5 | 30.0 |
| | $Li_2 + Li_5$ | 39.1 | 39.4 | 37.4 | 37.7 |
| | $Li_3 + Li_4$ | 46.5 | 46.4 | 44.6 | 44.5 |
| | 7Li | 158.7 | 161.6 | 148.8 | 151.7 |
| $Li_7^+$ | $Li + Li_6^+$ | 39.5 | 39.6 | 37.3 | 37.4 |
| | $Li_2 + Li_5^+$ | 40.0 | 40.2 | 38.9 | 39.1 |
| | $Li_3 + Li_4^+$ | 62.5 | 62.5 | 60.5 | 60.5 |
| | $Li_4 + Li_3^+$ | 48.6 | 48.8 | 47.4 | 47.6 |
| | $Li_5 + Li_2^+$ | 65.5 | 65.9 | 63.9 | 64.3 |
| | $Li_6 + Li^+$ | 61.2 | 61.7 | 61.8 | 62.3 |
| $Li_8$ | $Li + Li_7$ | 30.5 | 30.8 | 29.1 | 29.4 |
| | $Li_2 + Li_6$ | 34.8 | 34.9 | 34.8 | 34.9 |
| | $Li_3 + Li_5$ | 55.7 | 55.5 | 53.2 | 53.0 |
| | $2Li_4$ | 45.2 | 45.4 | 43.9 | 44.1 |
| | 8Li | 189.2 | 192.4 | 178.0 | 181.2 |
| $Li_8^+$ | $Li + Li_7^+$ | 20.9 | 20.7 | 21.7 | 21.5 |
| | $Li_2 + Li_6^+$ | 34.1 | 34.1 | 35.1 | 35.1 |
| | $Li_3 + Li_5^+$ | 47.0 | 46.6 | 47.3 | 46.9 |
| | $Li_4 + Li_4^+$ | 51.6 | 51.8 | 52.4 | 52.6 |
| | $Li_5 + Li_3^+$ | 48.2 | 48.2 | 48.6 | 48.6 |
| | $Li_6 + Li_2^+$ | 51.6 | 51.7 | 54.0 | 54.1 |
| | $Li_7 + Li^+$ | 51.5 | 51.7 | 54.0 | 54.2 |

[a] Ground electronic states assumed for all species.

**Table 4. Calculated Heats of Formation ($\Delta_f H$, kcal/mol) for the Lowest-Energy Isomers of $Li_nB^{0/+}$ at 0 and 298 K at the G3B3 and CCSD(T)/CBS Levels[a,b]**

| molecule | label | $\Delta_f H$ (0 K) CBS | $\Delta_f H$ (0 K) G3B3 | $\Delta_f H$ (298 K) CBS | $\Delta_f H$ (298 K) G3B3 |
|---|---|---|---|---|---|
| LiB ($^3\Pi$) | **B1** | 144.8 | 143.0 | 145.6 | 143.8 |
| $Li_2B$ ($^4A_2$) | **B2.1** | 145.6 | 143.1 | 146.1 | 143.6 |
| $Li_3B$ ($^1A_1$) | **B3.1** | 148.7 | 144.7 | 149.2 | 145.2 |
| $Li_4B$ ($^2B_2$) | **B4.1** | 140.8 | 139.1 | 141.1 | 139.4 |
| $Li_5B$ ($^1A_1$) | **B5.1** | 126.5 | 119.3 | 126.4 | 119.2 |
| $Li_6B$ ($^2A_{1g}$) | **B6.1** | 117.6 | 112.3 | 117.2 | 111.9 |
| $Li_7B$ ($^1A_1'$) | **B7.1** | 126.6 | 117.3 | 126.3 | 117.0 |
| $Li_8B$ ($^2A'$) | **B8.1** | 149.2 | 138.8 | 148.9 | 138.5 |
| $LiB^+$ ($^2\Sigma^+$) | **B1c** | 278.5 | 277.8 | 279.4 | 278.7 |
| $Li_2B^+$ ($^1\Sigma_g^+$) | **B2c.1** | 250.6 | 249.9 | 251.2 | 250.5 |
| $Li_3B^+$ ($^4A_2''$) | **B3c.1** | 244.2 | 241.8 | 244.8 | 242.4 |
| $Li_4B^+$ ($^1A_{1g}$) | **B4c.1** | 237.1 | 234.8 | 237.2 | 234.9 |
| $Li_5B^+$ ($^2A_1$) | **B5c.1** | 227.0 | 223.0 | 227.0 | 223.0 |
| $Li_6B^+$ ($^1A_{1g}$) | **B6c.1** | 206.6 | 201.1 | 206.0 | 200.5 |
| $Li_7B^+$ ($^2A_1'$) | **B7c.1** | 225.6 | 219.5 | 225.3 | 219.2 |
| $Li_8B^+$ ($^1A_1$) | **B8c.1** | 236.8 | 225.8 | 236.4 | 225.4 |

[a] Includes core−valence and scalar relativistic corrections and zero-point energies. [b] The ion heats of formation at 298 K were calculated in the ion convention where the electron has 0 kcal/mol for the integrated heat capacity of the electron.

($^3\Pi$) with a positive charge of 0.74 e on Li, which suggests B in LiB ($^3\Pi$) is in the $^3$P state of its anion $B^-$. At the CCSD(T)/CBS level, the bond dissociation energy of LiB ($^3\Pi$) is 28.0 kcal/mol, which is much larger than that of 18.5 kcal/mol for $LiB^+$ ($^2\Sigma^+$). The adiabatic ionization energy of LiB of 5.80 eV (CCSD(T)/CBS) is the highest of all of the $Li_nB$ clusters studied.

**$Li_2B$ and $Li_2B^+$.** Nguyen et al.[47] and Li et al.[46] reported that the ground state of $Li_2B$ is the $^2B_2$ state of $C_{2v}$ symmetry (**B2.2**). We find, at the CCSD(T)/CBS level, the high-spin $^4A_2$ state of $C_{2v}$ symmetry (**B2.1**) to be its ground state, which has not been reported previously to our knowledge. The low-spin $^2\Pi$ (**B2.2**, $D_{\infty h}$) and $^2B_2$ (**B2.3**, $C_{2v}$) states of $Li_2B$ are higher in energy than the $^4A_2$ state by 1.3 and 7.6 kcal/mol, respectively, at the B3LYP/aug-cc-pVTZ level. At the CCSD(T)/CBS level, the $^2\Pi$ state is higher in energy than the $^4A_2$ state by 4.0 kcal/mol. The $^2\Pi$ state has an electron configuration of $(1\sigma_g^+)^2(1\sigma_u^+)^2(2\sigma_g^+)^2(3\sigma_g^+)^2(2\sigma_u^+)^2(1\pi_u)^1$.

The ground state of $Li_2B^+$ is the $^1\Sigma_g^+$ state of $D_{\infty h}$ symmetry (**B2c.1**), which is derived from the $^2\Pi$ state by removing an electron from the $1\pi_u$ orbital. The $^3\Pi_g$ state, previously reported to be the most stable isomer,[45] is predicted to be 7.6 kcal/mol higher in energy than the $^1\Sigma_g^+$ state at the CCSD(T)/CBS level. The $^3\Pi_g$ state has an electron configuration of $(1\sigma_g^+)^2(1\sigma_u^+)^2(2\sigma_g^+)^2(3\sigma_g^+)^2(2\sigma_u^+)^1(1\pi_u)^1$. The Li−B distance of the $^1\Sigma_g^+$ state of 2.301 Å is slightly longer than that of the $^3\Pi_g$ state of 2.240 Å at the CCSD(T)/aVQZ level, and the symmetric stretching frequency of the $^1\Sigma_g^+$ state of 384 $cm^{-1}$ is also slightly larger than that of the $^3\Pi_g$ state of 371 $cm^{-1}$. The reaction energy for $Li_2B^+$ ($^1\Sigma_g^+$) → LiB ($^3\Pi$) + $Li^+$ ($^1$S) is predicted to be 56.1 kcal/mol.

The adiabatic ionization energy of $Li_2B$ is calculated as the energy difference between **B2.1** ($^4A_2$) and **B2c.1** ($^1\Sigma_g^+$) and is

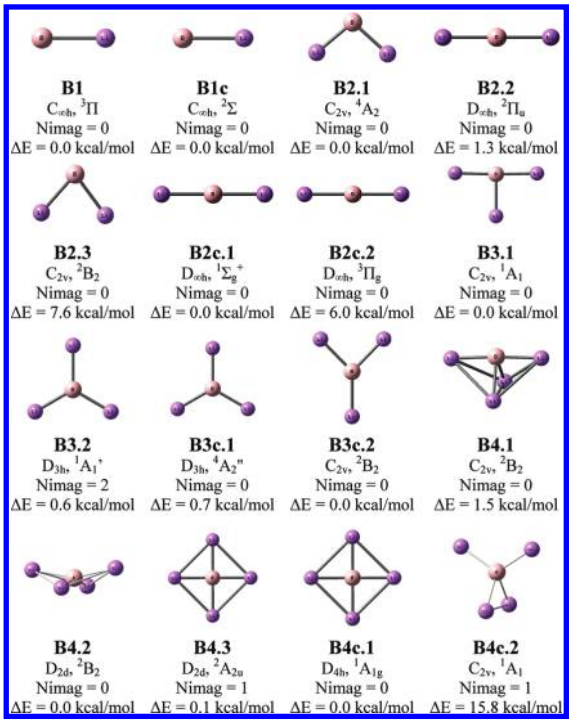


**Figure 4.** Optimized structures for $Li_nB$ ($n = 1-4$) and their cations and relative energies at 0 K ($\Delta E$, kcal/mol) calculated at the B3LYP/aVTZ level.

4.55 eV at the CCSD(T)/CBS level and 4.63 eV at the G3B3 level. The vertical ionization energy ($IE_v$) between **B2.1** and **B2c.1** of 5.11 eV (CCSD(T)/aVTZ) is markedly larger, consistent with the significant changes in the equilibrium geometries upon ionization. As ionization occurs between states with a difference in their multiplicity of ±1, we also calculated the adiabatic ionization energy as the energy difference between **B2.1** ($^4A_2$) and **B2c.2** ($^3\Pi_g$), which is predicted to be 4.88 eV at the CCSD(T)/CBS level.

**$Li_3B$ and $Li_3B^+$.** For $Li_3B$, our predictions are in qualitative agreement with previous results[45,47] in that **B3.1** ($C_{2v}$, $^1A_1$) is the most stable neutral isomer (Figure 4). **B3.2** ($D_{3h}$, $^1A_1'$) is a second-order saddle point with two imaginary frequencies, both of ~30i $cm^{-1}$, and is 2.2 kcal/mol higher in energy at 0 K (CCSD(T)/CBS). The CCSD(T)/aVQZ bond lengths for the ground state of $Li_3B$ (Li−B: 2.200 and 2.308 Å) are somewhat longer than that of the $^3\Pi$ state of LiB (2.146 Å).

**B3c.2** ($C_{2v}$, $^2B_2$) was reported to be the ground state of $Li_3B^+$.[46] At the B3LYP/aug-cc-pVTZ level, high-spin state **B3c.1** ($D_{3h}$, $^4A_2''$) is predicted to be 0.7 kcal/mol higher in energy than low-spin state **B3c.2**. However, at the CCSD(T)/CBS level, **B3c.1** is predicted to be lower in energy than **B3c.2** by 3.4 kcal/mol. The adiabatic ionization energy of $Li_3B$ (the energy difference between **B3.1** and **B3c.2**) is 4.14 eV at the CCSD(T)/CBS level. The corresponding vertical ionization energy at the CCSD(T)/aVTZ level is much larger, 4.60 eV. The ionization energy calculated from the energy difference between **B3.1** and **B3c.1** is 4.29 eV.

**$Li_4B$ and $Li_4B^+$.** The ground state of $Li_4B$ was previously predicted to be **B4.2** ($D_{2d}$, $^2B_2$) at the CCSD(T)/aug-cc-pVDZ,[46] B3LYP, and G2MP2 levels.[47] Our B3LYP/aug-cc-pVTZ results are consistent with these results. **B4.2** results from a small out-of-plane distortion of square planar structure **B4.3** ($D_{4h}$, $^2A_{2u}$), which was predicted to lie higher in energy than **B4.2** by 0.1 kcal/mol and to have one imaginary frequency of 32i $cm^{-1}$ at the B3LYP/augg-cc-pVTZ level. Thus, it is a transition state for the inversion of **B4.2**. At this DFT level of theory, **B4.1** ($C_{2v}$, $^2B_2$), which is derived from the further out-of-plane distortion of **B4.2**, was predicted to lie higher in energy than **B4.2** by 1.5 kcal/mol. However, at the CCSD(T)/CBS level with ZPE corrections calculated at the B3LYP/aug-cc-pVTZ level, **B4.1** is found to be the ground state of $Li_4B$, with **B4.2** and **B4.3** lying only 0.2 and 0.6 kcal/mol higher in energy, respectively. Thus, there are three different conformers related to the inversion distortion of planar **B4.3**. The low inversion barrier for **B4.1** at the CCSD(T) level means that the molecule will be very floppy and would probably have an average planar structure under most experimental conditions. The Li−B distances for **B4.1** (2.162 and 2.209 Å, CCSD(T)/aVQZ) are similar to that for the $^3\Pi$ state of LiB (2.146 Å).

**B4c.1** ($D_{4h}$, $^1A_{1\,g}$) is predicted to be the ground state of $Li_4B^+$, consistent with the previous CCSD(T)/6-311+G(d) study.[45] There is a substantial difference between the adiabatic and vertical ionization energies for the transition from **B4.1** to **B4c.1** for $Li_4B$ as a result of the large changes in equilibrium geometries as shown in Table 5.

**$Li_5B$ and $Li_5B^+$:** Structure B5.1 ($C_{4v}$, $^1A_1$) is predicted to be the neutral ground state (Figure 5). At the B3LYP/aug-cc-pVTZ level, structures **B5.2** ($D_{3h}$, $^2A_1'$) and **B5.3** ($C_{2v}$, $^2A_1$) are predicted to be transition states with essentially the same energy, 1.5 kcal/mol higher than that of **B5.1**. The Li−B distances for **B5.1** (2.150 and 2.228 Å) are similar to that for the $^3\Pi$ state of LiB (2.146 Å).

The removal of an electron from the HOMO of the neutral cluster does not substantially affect the equilibrium geometry, and **B5c.1** ($C_{4v}$, $^2A_1$) is predicted to be the ground state of the cation. Consistent with the modest changes in the equilibrium geometry, there is little difference betweeen the adiabatic and vertical ionization energies for $Li_5B$ as shown in Table 5.

**$Li_6B$ and $Li_6B^+$.** In agreement with earlier studies,[46,47] **B6.1** ($O_h$, $^2A_{1g}$) is predicted to be the ground state for $Li_6B$ (Figure 5). At the CCSD(T)/aVTZ level, the Li−B bond lengths in **B6.1** are calculated to be 2.182, which is slightly longer than that for the $^3\Pi$ state of LiB (2.152 Å) calculated at the same level of theory.

**B6c.1** ($O_h$, $^1A_{1g}$) is predicted to be the ground state for $Li_6B^+$, consistent with previous studies.[46,47] At the CCSD(T)/aVTZ level, the Li−B bond lengths in **B6c.1** are calculated to be 2.197 Å, slightly longer than the value in **B6.1**. Because of the small changes in the equilibrium geometries, there is little difference between the adiabatic and vertical ionization energies for $Li_6B$ as shown in Table 5. The adiabatic ionization energy is predicted to be 3.86 eV at the CCSD(T)/CBS level, which is lower than for the $Li_nB$ clusters for $n = 1$ to 5 and 7.

**$Li_7B$ and $Li_7B^+$.** Our results are in agreement with previous reports[46,47] that pentagonal bipyramidal structure **B7.1** ($D_{5h}$, $^1A_1'$) is the ground state for $Li_7B$ (Figure 5). **B7.2** ($C_{3v}$, $^1A_1$) is predicted to be 4.4 kcal/mol higher in energy than **B7.1** at the B3LYP/aug-cc-pVTZ level. **B7.1** exhibits a HOMO−LUMO gap of 1.67 eV, which is larger than the corresponding gaps of 1.48 and 1.44 eV for $Li_3B$ and $Li_5B$, respectively.

Pentagonal bipyramidal structure **B7c.1** ($D_{5h}$, $^2A_1'$) is predicted to be the ground state for $Li_7B^+$.[46,47] Cationic structure **B7c.2** ($C_{3v}$, $^2A_1$) is predicted to be 3.4 kcal/mol higher in energy than **B7c.1**. Similar to $Li_6B$, there is little difference between the adiabatic and vertical ionization energies for $Li_7B$ as shown in Table 5.

**Table 5. Adiabatic and Vertical Ionization Energies ($IE_a$/$IE_v$, eV) using the CCSD(T)/aug-cc-pV*n*Z and G3B3 Methods and the HOMO(SOMO)−LUMO Gap (eV) of the Lowest Closed-Shell Isomers at the B3LYP/6-311+G(d) Level for the $Li_nB$ Clusters ($n$ = 1−8)**

| | | $IE_a$ | $IE_a$ | $IE_a$ | $IE_v$ | neutral | cation |
|---|---|---|---|---|---|---|---|
| neutral | cation | aVTZ | CBS | G3B3 | aVTZ | GAP | GAP |
| LiB ($C_{\infty v}$, $^3\Pi$) | $LiB^+$ ($C_{\infty v}$, $^2\Sigma^+$) | 5.72 | 5.80 | 5.84 | 5.89 | | |
| $Li_2B$ ($C_{2v}$, $^4A_2$) | $Li_2B^+$ ($D_{\infty h}$, $^1\Sigma_g^+$) | 4.52 | 4.55 | 4.63 | 5.11 | | 2.57 |
| $Li_2B$ ($C_{2v}$, $^4A_2$) | $Li_2B^+$ ($D_{\infty h}$, $^3\Pi_g$) | 4.80 | 4.88 | | | | |
| $Li_3B$ ($C_{2v}$, $^1A_1$) | $Li_3B^+$ ($D_{3h}$, $^4A_2''$) | 4.07 | 4.14 | 4.21 | 4.60 | 1.48 | |
| $Li_3B$ ($C_{2v}$, $^1A_1$) | $Li_3B^+$ ($C_{2v}$, $^2B_2$) | 4.24 | 4.29 | | | | |
| $Li_4B$ ($C_{2v}$, $^2B_2$) | $Li_4B^+$ ($D_{4h}$, $^1A_{1g}$) | 4.15 | 4.18 | 4.33 | 5.02 | | 2.16 |
| $Li_4B$ ($D_{2d}$, $^2B_2$) | $Li_4B^+$ ($D_{4h}$, $^1A_{1g}$) | 4.13 | 4.17 | | | | |
| $Li_5B$ ($C_{4v}$, $^1A_1$) | $Li_5B^+$ ($C_{4v}$, $^2A_1$) | 4.33 | 4.36 | 4.50 | 4.57 | 1.44 | |
| $Li_6B$ ($O_h$, $^2A_{1g}$) | $Li_6B^+$ ($O_h$, $^1A_{1g}$) | 3.85 | 3.86 | 3.85 | 3.84 | | 2.43 |
| $Li_7B$ ($D_{5h}$, $^1A_1'$) | $Li_7B^+$ ($D_{5h}$, $^2A_1'$) | 4.27 | 4.29 | 4.43 | 4.28 | 1.69 | |
| $Li_8B$ ($C_s$, $^2A'$) | $Li_8B^+$ ($D_{4d}$, $^1A_1$) | 3.80 | 3.80 | 3.83 | 3.85 | | 1.83 |

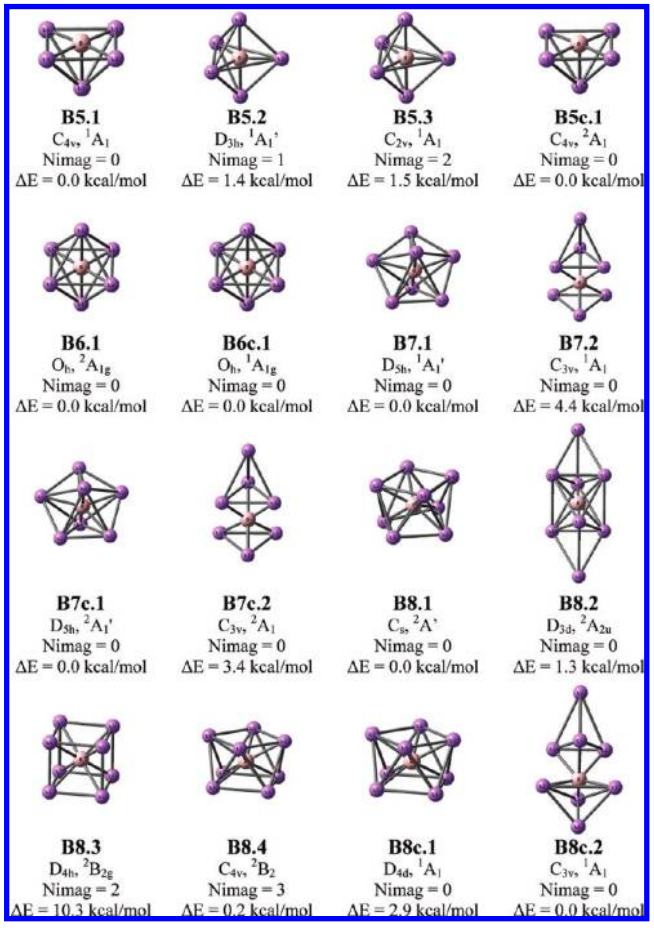


**Figure 5.** Optimized structures for $Li_nB$ ($n$ = 5−8) and their cations and relative energies at 0 K ($\Delta E$, kcal/mol) calculated at the B3LYP/aVTZ level.

**$Li_8B$ and $Li_8B^+$.** Different quantum chemical methods (B3LYP and MP2 with the 6-31G(d) basis set, and G2MP2)[47] predict two different structures for $Li_8B$, a $C_{3v}$ structure (similar to **B8.2** ($D_{3d}$)) in which the B atom is bonded to two distorted "tetrahedral" $Li_4$ units and a $D_{4h}$ structure **B8.3** where the B atom is located at the center of the $Li_8$ cube. The first structure was predicted to be 26.6 kcal/mol more stable than the second structure at the HF/6-31G(d) level. We searched for several possible structures of $Li_8B$ and $Li_8B^+$, and some low-energy forms are shown in Figure 5. They include the two earlier structures, namely **B8.2** ($D_{3d}$) and **B8.3** ($D_{4h}$), new $C_{4v}$ structure **B8.4**, a prismatic structure derived from the $D_{4h}$ structure, and new $C_s$ structure **B8.1** derived from a distortion of the $C_{4v}$ structure. At the CCSD(T)/aVTZ level, **B8.1** ($C_s$, $^2A'$) is calculated to be the ground state whereas **B8.2** ($D_{3d}$, $^2A_{2u}$) is predicted to be 15.9 kcal/mol higher in energy. **B8.4** ($C_{4v}$, $^2B_2$) is a saddle point with three imaginary frequencies, 9.6 kcal/mol higher than **B8.1** at the B3LYP/aug-cc-pVTZ level.

For the cation, **B8c.1** ($D_{4d}$, $^1A$) and **B8c.2** ($C_{3v}$, $^1A_1$) are predicted to be nearly degenerate, with an energy difference of only 1.5 kcal/mol (CCSD(T)/aVTZ). For both the neutral and cationic clusters, the high-symmetry $D_{4h}$ structure is a second-order saddle point. The adiabatic ionization energy of $Li_8B$ of 3.80 eV calculated at the CCSD(T)/CBS level is the smallest among all of the $Li_nB$ clusters studied.

## DISCUSSION

**Ionization Energies (IEs).** There is very good agreement between the experimental and calculated ionization energies for the $Li_n$ clusters. The calculated $IE_a$ values of 5.392 eV (CCSD(T)/CBS) and 5.40 eV (G3B3) of Li are in good agreement with the experimental value of 5.391719 eV.[84] For $Li_4$, the experimental spectrum[79b] was reassigned on the basis of the comparison of the experimental spectrum with our simulated photoionization efficiency spectrum. The previously reported ionization energy of 4.31 ± 0.05 eV for $Li_4$ is adjusted to 4.70 ± 0.05 eV. We note that previous calculations by Wheeler and Schaefer[14b] also indicate that the previously reported experimental value is a lower bound of the adiabatic ionization energy. Overall, the difference between our CCSD(T) results and the experimental values for the $IE_a$ values for the $Li_n$ clusters are less than 0.1 eV when the adjusted value for $Li_4$ is used. There is little difference between the IEs obtained at the CCSD(T)/CBS level with the core−valence and scalar relativistic corrections and at the CCSD(T)/cc-pVTZ level for $Li_n$. The maximum difference is


dx.doi.org/10.1021/jp200992u |J. Phys. Chem. A 2011, 115, 7673–7686

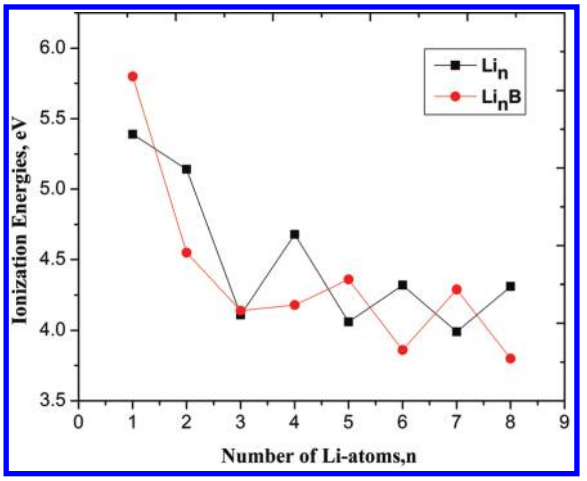


**Figure 6.** Adiabatic ionization energies of $Li_n$ and $BLi_n$ calculated by CCSD(T)/CBS.

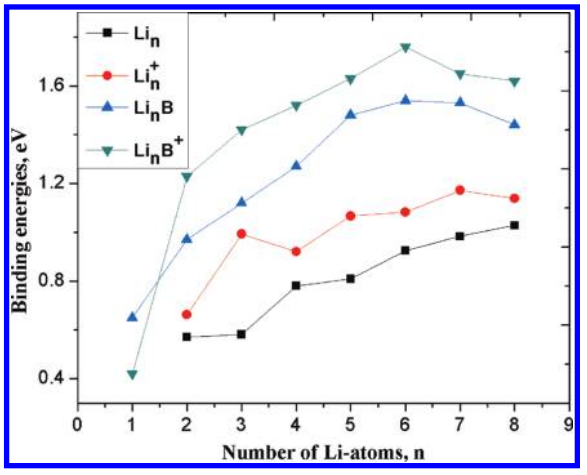


**Figure 7.** Average binding energy at 0 K in eV of $Li_n$ and $Li_nB$ ($n = 1-8$) in both neutral and cationic states calculated by G3B3.

0.05 eV. The G3B3 IEs are slightly larger. These results suggest that the ionization energies calculated for the $Li_nB$ clusters should be good to 0.1 eV.

The IEs plotted in Figure 6 for $Li_n$ and $Li_nB$ show an odd−even oscillation. For $Li_n$, the highest $IE_a$ is for the Li atom and the $IE_a$ generally decreases with increasing cluster size. It is easier to ionize the $Li_n$ clusters with an unpaired electron (excluding $n = 1$) than the clusters with even numbers of paired electrons. This difference is on the order of 0.3 eV for the larger clusters. The $IE_a$ values of $Li_6$ and $Li_8$ are comparable at 4.3 eV and are still far from the work function of the metal of 2.93 eV.[85]

For the $Li_nB$ clusters, the $IE_a$ values for the same number of Li atoms show the opposite trend (Figure 6) in terms of even−odd alternation because the additional B atom makes the odd number of $Li_n$ clusters closed shell and the even number of $Li_n$ clusters open shell. The effect of the B atom can be to raise or lower the $IE_a$. For LiB, the $IE_a$ is substantially increased as compared to that for Li, but for $Li_2B$, the $IE_a$ is decreased as compared to that for $Li_2$. For $Li_3B$ and $Li_3$, the $IE_a$ values are the same, and for $n = 4$, the $IE_a$ of $Li_4B$ is substantially lower than that of $Li_4$. For $n = 5$ and 7, the $IE_a$ of $Li_n$ is lower than that of $Li_nB$, but the opposite is true for $n = 6$ and 8. Thus, in general, the structures with an unpaired electron are more readily ionized than those with paired electrons and the $IE_a$ decreases as the cluster size increase, consistent with the ability of the cluster to delocalize the positive charge.

**Clustering Energies.** The relative stabilities of both series of clusters and their cations can be examined on the basis of the normalized binding energy ($E_b$) and the second-order difference in the total energies ($\Delta^2E$). For $Li_n$ and $Li_n^+$, we define

$$E_b(Li_n) = \frac{nE(Li) - E(Li_n)}{n} \quad (1)$$

$$E_b(Li_n^+) = \frac{(n\text{-}1)E(Li) + E(Li^+) - E(Li_n^+)}{n} \quad (2)$$

$$\Delta^2E(Li_n) = E(Li_{n-1}) + E(Li_{n+1}) - 2E(Li_n) \quad (3)$$

$$\Delta^2E(Li_n^+) = E(Li_{n-1}^+) + E(Li_{n+1}^+) - 2E(Li_n^+) \quad (4)$$

For $Li_nB$ and $Li_nB^+$, we define

$$E_b(Li_nB) = \frac{nE(Li) + E(B) - E(Li_nB)}{n+1} \quad (5)$$

$$E_b(Li_nB^+) = \frac{(n-1)E(Li) + E(Li^+) + E(B) - E(Li_nB^+)}{n+1} \quad (6)$$

$$\Delta^2E(Li_nB) = E(Li_{n-1}B) + E(Li_{n+1}B) - 2E(Li_nB) \quad (7)$$

$$\Delta^2E(Li_nB^+) = E(Li_{n-1}B^+) + E(Li_{n+1}B^+) - 2E(Li_nB^+) \quad (8)$$

The four normalized binding energies are compared in Figure 7. For $Li_n$, the normalized binding energies tend to increase with increasing cluster size, although for $n = 3$ and 5 (open-shell molecules) the normalized binding energy is not much larger than for $n = 2$ and 4, respectively. This is consistent with the behavior of odd and even binding energies often seen in small metallic clusters where the closed-shell species are more stable on a per atom basis than are the open-shell species.

The normalized binding energies of $Li_n^+$ show the opposite behavior in terms of even and odd numbers of atoms with a clear odd−even oscillation in which the cations bearing a closed-shell electron configuration ($n = 3$, 5, 7) have larger $E_b$ values. Doping the $Li_n$ cluster with one boron atom greatly increases its binding energy because of the increase in the number of chemical bonds and the larger bond energy of the Li−B bond as compared to that of the Li−Li bond. At the CCSD(T)/CBS level, the dissociation energy at 0 K of LiB is ~4 kcal/mol larger than that of $Li_2$.

The normalized binding energies of the cationic clusters are predicted to be larger than those of the corresponding neutral clusters in the pure and B-doped systems. This trend holds even in the case where the cation is open-shell (high-spin multiplicity) and the corresponding neutral is closed-shell (low-spin multiplicity). The size of the normalized binding energy apparently has more to do with the cluster size than with the spin multiplicity in terms of open- or closed-shell species.

Another possible comparison is given by the binding energy (BE) of an atom to a cluster, as shown in reaction 9 for $Li_n$ (BE1):

$$Li_n \rightarrow Li + Li_{n-1} \quad (9)$$


dx.doi.org/10.1021/jp200992u |J. Phys. Chem. A 2011, 115, 7673–7686

**Table 6. Calculated Dissociation Enthalpies (kcal/mol) of $Li_nB$ at 0 K at the CCSD(T)/CBS Level**

| molecule | label | reaction11a | reaction11b |
|---|---|---|---|
| LiB ($C_{\infty v}$, $^3\Pi$) | **B1** | 28.0 | 28.0 |
| $Li_2B$ ($C_{2v}$, $^4A_2$) | **B2.1** | 36.9 | 41.1 |
| $Li_3B$ ($C_{2v}$, $^1A_1$) | **B3.1** | 34.6 | 62.3 |
| $Li_4B$ ($C_{2v}$, $^2B_2$) | **B4.1** | 45.6 | 78.1 |
| $Li_5B$ ($C_{4v}$, $^1A_1$) | **B5.1** | 52.0 | 109.5 |
| $Li_6B$ ($O_h$, $^2A_{1g}$) | **B6.1** | 46.7 | 124.4 |
| $Li_7B$ ($D_{5h}$, $^1A_1'$) | **B7.1** | 28.6 | 123.5 |
| $Li_8B$ ($C_s$, $^2A'$) | **B8.1** | 15.1 | 109.5 |

**Table 7. Calculated Dissociation Enthalpies (kcal/mol) of $Li_nB^+$ at 0 K at the CCSD(T)/CBS Level**

| molecule | label | reaction12a | reaction12b |
|---|---|---|---|
| $LiB^+$ ($C_{\infty v}$, $^2\Sigma^+$) | **B1c** | | 18.5 |
| $Li_2B^+$ ($D_{\infty h}$, $^1\Sigma_g^+$) | **B2c.1** | 65.6 | 56.1 |
| $Li_3B^+$ ($D_{3h}$, $^4A_2''$) | **B3c.1** | 44.1 | 63.3 |
| $Li_4B^+$ ($D_{4h}$, $^1A_{1g}$) | **B4c.1** | 44.8 | 73.5 |
| $Li_5B^+$ ($C_{4v}$, $^2A_1$) | **B5c.1** | 47.8 | 75.7 |
| $Li_6B^+$ ($O_h$, $^1A_{1g}$) | **B6c.1** | 58.2 | 81.9 |
| $Li_7B^+$ ($D_{5h}$, $^2A_1'$) | **B7c.1** | 18.6 | 53.8 |
| $Li_8B^+$ ($D_{4d}$, $^1A_1$) | **B8c.1** | 26.6 | 51.8 |

These values correspond to the cohesive energy of the cluster. The values (Table 3) show an even−odd oscillation for $n = 2$ and 3 and $n = 4$ and 5. However, the value is approximately converged at 30 to 32 kcal/mol at $n = 4$. This value can be compared to the cohesive energy of Li of 37.7 ± 0.2 kcal/mol.[68] Of interest is the fact that the highest value for BE1 is for $n = 6$.

The BE for the cations can be defined by reaction 10a (BE2) and reaction 10b (BE3):

$$Li_n^+ \rightarrow Li^+ + Li_{n-1} \quad (10a)$$

$$\rightarrow Li + Li_{n-1}^+ \quad (10b)$$

BE1 shows an increase from $n = 2$ to 7 and a decrease at $n = 8$. BE2 shows a substantial decrease for $n = 4$ and 8 with a smaller decrease for $n = 6$. As expected, BE2 is larger than BE3 because of the ability of the cluster in reaction 10b to delocalize the positive charge better. We note that the BE2 values can be quite low, especially for the even number of clusters, and it will be relatively easy to remove an Li atom from the positively charged cluster. These results, coupled with the value of the BE for $Li_8$, suggest that $Li_6$ is a very stable species and that $Li_8$ is less stable.

Corresponding binding energies BE4 and BE5 for the neutral boron clusters are given in reactions 11a and 11b (Table 6).

$$Li_nB \rightarrow Li_{n-1}B + Li \quad (11a)$$

$$\rightarrow Li_n + B \quad (11b)$$

The energy required to lose a Li atom (eq 11a) is less than that for the loss of a B atom, excluding LiB. The loss of a Li atom essentially increases to $n = 5$ and then decreases to $n = 8$, where the loss of Li is expected to cost only 15 kcal/mol. The value of BE5 is substantially larger than for BE4, increasing to ~124 kcal/mol for $n = 6$ and 7. The value of BE5 decreases for $n = 8$.

For $Li_nB^+$, the two dissociation channels are given by reactions 12a (BE6) and 12b (BE7, Table 7).

$$Li_nB^+ \rightarrow Li_{n-1}B^+ + Li \quad (12a)$$

$$\rightarrow Li_{n-1}B + Li^+ \quad (12b)$$

Except for $Li_2B^+$, the loss of Li is favored over the loss of $Li^+$, presumably because of the ability of the larger cluster to stabilize the positive charge. The largest value for BE6 is for $Li_2B^+$, and the lowest is 19 kcal/mol for $Li_7B^+$. Excluding $LiB^+$, the values for BE7 range from 52 to 82 kcal/mol. The largest values for BE6 and for BE7 are for $Li_6B^+$. This suggests that $Li_6B^+$ has additional stability, consistent with the low ionization potential of $Li_6B$. It is interesting that $Li_6B$ is also a very stable species as shown by comparing its binding energy with those of $Li_5B$ and $Li_7B$. The second-order energy differences are displayed in Figure 8 for the larger clusters. The remarkably large value identified for $Li_6B^+$ is consistent with a higher stability as compared to other members of the series, especially given that $Li_6B$ is not strongly destabilized.

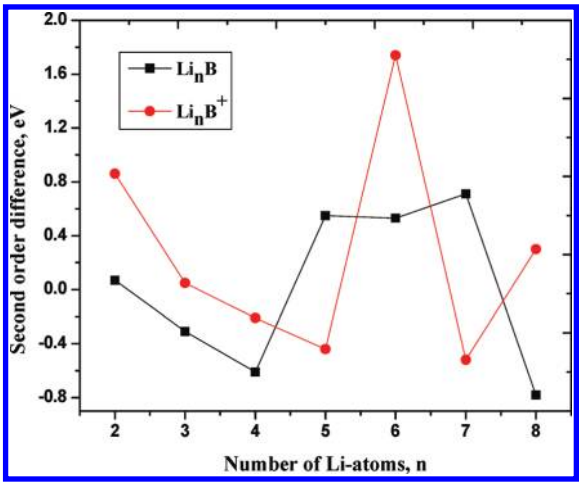


**Figure 8.** Second-order difference of the average binding energy at 0 K in eV of the $Li_nB$ clusters in both neutral and cationic states as calculated by G3B3.

**Growth Mechanism.** In Figures 1−4, it is obvious that the $Li_nB$ cluster is constructed by bonding the new Li to the B on $Li_{n-1}B$. There is a tendency to increase the coordination number of the B atom (i.e., binding Li to B of diatomic LiB to form triatomic $Li_2B$). For $n \geq 6$, B prefers a central position of the lithium cluster to form higher-symmetry structures such as $Li_6B$ ($O_h$) and $Li_7B$ ($D_{5h}$). Structures **B8.2** ($D_{3d}$) and **B8.1** ($C_s$), which have coordination numbers of six and eight, respectively, are the lowest neutral isomers, and their cationic counterparts are almost degenerate in energy. **B8.2** ($D_{3d}$) is formed by adding Li to a $Li_3$ face of a "tetrahedral" $Li_4$ unit of $Li_7B$ ($C_{3v}$). A direct connection of one Li to B of $Li_7B$ ($D_{5h}$) gives rise to the latter. For the neutrals, the first addition mode is somewhat preferred over the second, consistent with the fact that the Li−B bond is stronger as compared to the Li−Li bond. We predict that the larger clusters $Li_nB$ ($n \geq 9$) likely prefer the first growth mode for the most stable clusters.

**Electron Localization Function (ELF).** The ELF plots for some selected structures including $Li_5B$, $Li_6B^+$, $Li_7B$, and $Li_8B^+$ are displayed in Figure 9. There is perfect electron delocalization in these systems. The ELF analysis of $Li_5B$ (**B5.1**) shows four

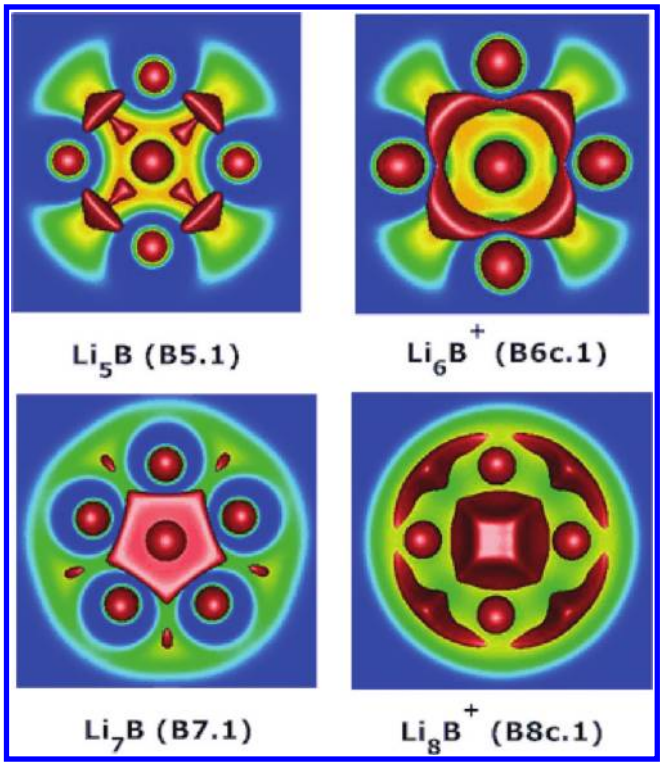


**Figure 9.** ELF plots of high-stability species $Li_5B$, $Li_6B^{\pm}$, $Li_7B$, and $Li_8B^+$.

trisynaptic (Li−Li−Li) basins, each containing ∼1.9 electrons. This indicates the emergence of three-center−two-electron (3c−2e) bonds. Similarly, the ELF plot for $Li_6B^+$ (**B6c.1**) points out the existence of eight trisynaptic (Li−Li−Li) basins, each of which contains ∼1.0 electron. These populations confirm the presence of multicenter bonds, and also a global electron delocalization in **B6c.1** that lends further support to its high stability.

Similar observations are found for the other members $Li_7B$ and $Li_8B^+$. The ELF plot of $Li_7B$ (**B7.1**) reveals a perfect electron delocalization in which electrons are mainly distributed on basins of triangle $Li_3$ whereas the electrons of $Li_8B^+$ (**B8c.1**) are globally populated on eight trisynaptic basins, that again suggest the existence of three-center bonds and strong electron delocalization.

**Phenomenological Shell Model (PSM).** The stability pattern of the $Li_nB$ clusters can be further probed within the framework of the PSM. This model was proposed by Knight et al.[49] to interpret the stability pattern and electronic structure of simple metal clusters.[86−88] In the framework of this model, the valence electrons are assumed to be freely itinerant in a simple mean-field potential formed by the nuclei. A very stable metal cluster is predicted if its electronic shell or subshells are closed; the numbers of valence electrons corresponding to shell closings such as $2(1s^2)$, $8(1s^21p^6)$, and $20(1s^21p^61d^{10}2s^2)$ are called magic numbers. We note that the notation for shells 1p, 1d,... are from the PSM and do not correspond to the actual molecular orbitals. In binary clusters, the number of valence electrons does not always correspond to a magic number (e.g., $K_8Zn$,[89] $Na_6Pb$,[90]...). A modified potential was subsequently introduced to account for the behavior of these cases.[91,92] According to the modified model, the dopant induces a slight perturbation and the

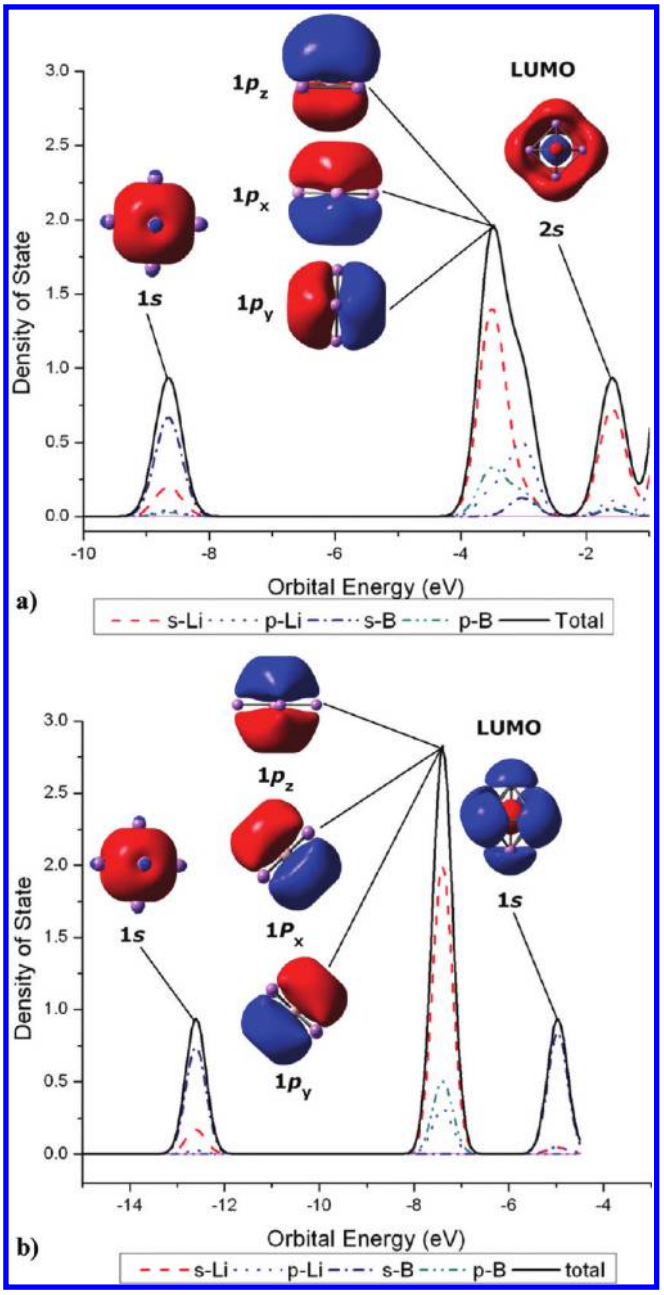


**Figure 10.** Plot of the density of states of (a) $Li_5B$ (**B5.1**) and (b) $Li_6B^+$ (**B6c.1**) using the calculated orbitals at the B3LYP/6-311+G(d) level.

ordering of the single-particle energy levels is changed either to $(1s^21p^62s^21d^{10}2p^6)$ if the impurity is more electronegative than the host atoms or to $(1s^21p^61d^{10}2s^21f^{14}2p^6)$ if the central dopant is less electronegative than the host atoms. In the present case, the B impurity plays the role of an electronegative dopant for the Li clusters.

The energetic ordering of molecular orbitals can be correlated with the PSM using the modified potential version. (See the Supporting Information for diagrams of closed-shell Kohn−Sham orbitals from the B3LYP calculations.) As examples, we examine high-stability, closed-shell species $Li_5B$, $Li_6B^+$, $Li_7B$, and $Li_8B^+$. The approximate density of states derived from the B3LYP Kohn−Sham orbitals of $Li_5B$ and $Li_6B^+$ is depicted in Figure 10. Neutral $Li_5B$ has eight valence electrons, and its shell is

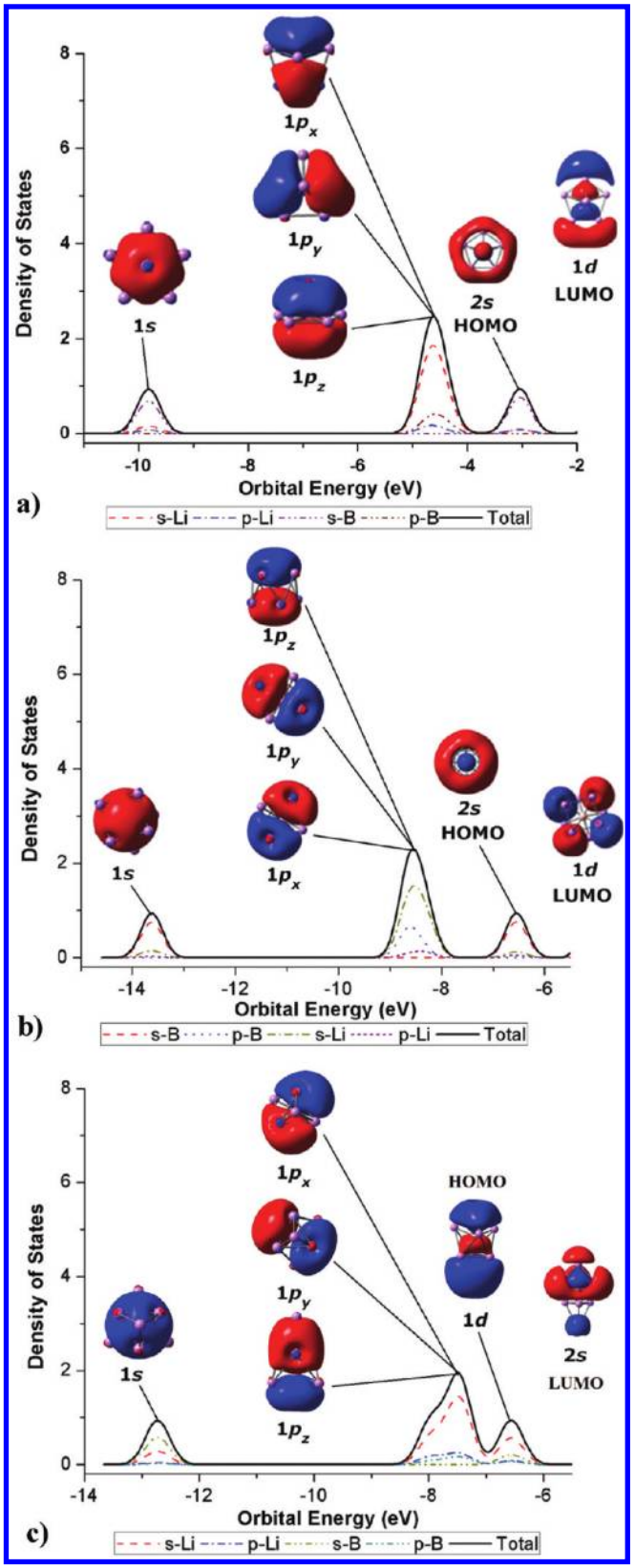


**Figure 11.** Plot of the density of states of (a) $Li_7B$ (**B7.1**), (b) $Li_8B^+$ (**B8c.1**), and (c) $Li_8B^+$ (**B8c.2**) using the calculated orbitals at the B3LYP/6-311+G(d) level.

closed. Three orbitals (HOMO, degenerate HOMO-1, Figure 10) for $Li_5B$ have p character, and HOMO-2 is an s orbital. Thus, $Li_5B$ is consistent with the configuration $(1s^21p^6)$ of the PSM. A similar observation can be made for isoelectronic $Li_6B^+$ (Figure 10), whose shell is also closed with eight valence electrons filling the $(1s^21p^6)$ configuration. Consequently, $Li_5B$ has a higher adiabatic ionization energy of 4.36 eV than that of 3.86 eV for $Li_6B$ (CCSD(T)/CBS). The LUMO in both species is an s orbital, consistent with the energy ordering of $(1s^21p^62s^01d^0)$ (with a modified potential) instead of level $(1s^21p^61d^02s^0)$ of the simple PSM, consistent with B being more electronegative than Li.

Neutral $Li_7B$ has 10 valence electrons. Its HOMO and HOMO-3 are s orbitals, HOMO-1 can be considered to be a $p_z$ orbital, and degenerate HOMO-2 corresponds to the $p_x$ and $p_y$ orbitals. Consequently, its LUMO according to the PSM model should be a d-type orbital as shown in Figure 11. $Li_8B^+$ has two structures **B8c.1** ($D_{4d}$, $^1A_1$) and **B8c.2** ($C_{3v}$, $^1A_1$) of nearly the same energy. **B8c.1** is consistent with a configuration of $(1s^21p^62s^21d^0)$ as shown in Figure 11, but **B8c.2** is consistent with the arrangement of $(1s^21p^61d^22s^0)$. Thus, structure **B8c.2** can be considered to be distorted geometry and is better interpreted by using the Clemenger−Nilsson model.[93]

## CONCLUSIONS

We predicted the electronic structures, stabilities, and thermochemical properties of small, pure lithium clusters $Li_n$, B-doped lithium clusters $Li_nB$, and their cations using DFT, CCSD(T)/CBS, and G3B3. Extensive searches for possible structures were carried out, and previous global minima are confirmed or new ones identified. Heats of formation ($\Delta_fH$) are calculated from the total atomic energies (TAE) using the composite G3B3 model and the highly accurate CCSD(T)/CBS method. Calculated adiabatic ionization energies ($IE_a$) agree well with available experimental data. For $Li_4$, we reassigned the experimental $IE_a$ to 4.70 eV on the basis of our calculated $IE_a$ and simulated spectrum. The CCSD(T)/CBS values are closer to experiment than the G3B3 values. Species such as $Li_5B$, $Li_6B^+$, $Li_7B$, and $Li_8B^+$ are characterized by a higher stability as compared to that of their neighbors, which can be explained by the magic numbers of the phenomenological shell model.

## ASSOCIATED CONTENT

**Supporting Information.** Energies and equilibrium geometries calculated at the B3LYP/aug-cc-pVTZ level. Energy contributions and equilibrium geometries calculated at the CCSD(T) level. Kohn−Sham orbitals for the closed-shell clusters. This material is available free of charge via the Internet at http://pubs.acs.org.

## AUTHOR INFORMATION

### Corresponding Author

*E-mail: minh.nguyen@chem.kuleuven.be; dadixon@bama.ua.edu.

## ACKNOWLEDGMENT

M.T.N. is indebted to the K.U. Leuven Research Council for support (GOA, IDO, and IUAP programs). T.B.T. thanks the Arenberg Doctoral School for a scholarship. This work was supported in part by the Chemical Sciences, Geosciences and Biosciences Division, Office of Basic Energy Sciences, U.S. Department of Energy (DOE) under grant no. DE-FG02-

03ER15481 (catalysis center program). D.A.D. also thanks the Robert Ramsay Chair Fund of The University of Alabama for support.

## REFERENCES

(1) (a) Wu, C. H. *J. Chem. Phys.* **1976**, *65*, 3181. (b) Wu, C. H. *J. Phys. Chem.* **1983**, *87*, 1534.
(2) Brechihnac, C.; Busch, H.; Cahuzac, P.; Leygnier, J. *J. Chem. Phys.* **1994**, *101*, 6992.
(3) Kornath, A.; Kaufmann, A.; Zoermer, A.; Ludwig, R. *J. Chem. Phys.* **2003**, *118*, 6957.
(4) (a) Blanc, J.; Bonacic-Koutecky, V.; Broyer, M.; Chevaleyre, J.; Dugourd, P. *J. Chem. Phys.* **1992**, *96*, 1793. (b) Dugourd, P.; Chevaleyre, J.; Broyer, M.; Wolf, J.; Woste, L. *Chem. Phys. Lett.* **1990**, *175*, 555.
(5) Sarkas, H. W.; Arnold, S. T.; Hendrickx, J. H.; Bowen, K. H. *J. Chem. Phys.* **1995**, *103*, 2653.
(6) Boldyrev, A. I.; Simons, J.; Schleyer, P. v. R. *J. Chem. Phys.* **1993**, *99*, 8793.
(7) Alexandrova, A. N.; Boldyrev, A. I. *J. Chem. Theory Comput.* **2005**, *1*, 566.
(8) Boustani, I.; Koutecky, J. *J. Chem. Phys.* **1998**, *88*, 5657.
(9) Boustani, I.; Pewestort, W.; Fantucci, P.; Bonacic-Koutecky, V.; Koutecky, J. *Phys. Rev. B* **1987**, *35*, 9437.
(10) Jones, R. O.; Lichtenstein, A. I.; Hutter, J. *J. Chem. Phys.* **1997**, *106*, 4566.
(11) (a) Rao, K.; Khanna, S. N.; Jena, P. *Phys. Rev. B* **1987**, *36*, 953. (b) Rao, K.; Khanna, S. N.; Jena, P. *Phys. Rev. B* **1991**, *43*, 1416.
(12) Gardet, G.; Rogemond, F.; Chermette, H. *J. Chem. Phys.* **1996**, *105*, 9933.
(13) Fournier, R.; Joey, C. J.; Wong, A. *J. Chem. Phys.* **2003**, *119*, 9444.
(14) (a) Wheeler, S. E.; Sattelmeyer, K. W.; Schleyer, P. V. R.; Schaefer, H. F.; Wu, C. H. *J. Chem. Phys.* **2004**, *120*, 4683. (b) Wheeler, S. E.; Schaefer, H. F., III. *J. Chem. Phys.* **2005**, *122*, 204328.
(15) Temelso, B.; Sherrill, C. D. *J. Chem. Phys.* **2005**, *112*, 064315.
(16) Kawai, R.; Tombrello, J. F.; Weare, J. H. *Phys. Rev. A* **1994**, *49*, 4236.
(17) Visser, S. P.; Alpert, Y.; Danovich, D.; Shaik, S. *J. Phys. Chem. A* **2000**, *104*, 11223.
(18) (a) Reichardt, V.; Bonacic-Koutecky, V.; Fantucci, P.; Jellinek, J. *Chem. Phys. Lett.* **1997**, *279*, 129. (b) Bonacic-Kouteky, V.; Pittner, J.; Koutecky, J. *J. Chem. Phys.* **1996**, *210*, 313.
(19) (a) Dixon, D. A.; Gole, J. L.; Jordan, K. D. *J. Chem. Phys.* **1997**, *66*, 567. (b) Gole, J. L.; Childs, R. H.; Dixon, D. A.; Eades, R. A. *J. Chem. Phys.* **1980**, *72*, 6368. (c) Richtsmeier, S. C.; Eades, R. A.; Dixon, D. A.; Gole, J. L. In *Metal Bonding and Interactions in High Temperature Systems*; ACS Symposium Series; Gole, J. L., Stwalley, W. C., Eds.; American Chemical Society: Washington, DC, 1982; Vol. 179, p 177. (d) Eades, R. A.; Hendewerk, M. L.; Frey, R.; Dixon, D. A.; Gole, J. L. *J. Chem. Phys.* **1982**, *76*, 3075. (e) Richtsmeier, S. C.; Dixon, D. A.; Gole, J. L. *J. Phys. Chem.* **1982**, *86*, 3942.
(20) (a) Wu, C. H.; Kudo, H.; Ihle, H. R. *J. Chem. Phys.* **1997**, *70*, 1534. (b) Wu, C. H. *Chem. Phys. Lett.* **1987**, *139*, 357.
(21) Jiang, Z. Y.; Lee, K. H.; Li, S. T.; Chu, S. Y. *Int. J. Mass Spectrosc.* **2006**, *253*, 104.
(22) Deshpande, M. D.; Kanhere, D. G. *Phys. Rev. A* **2002**, *65*, 033202.
(23) Baruah, T.; Kanhere, D. G. *Phys. Rev. A* **2001**, *63*, 063202.
(24) Deshpande, M.; Dhavale, A.; Zope, R. R.; Chacko, S.; Kanhere, D. G. *Phys. Rev. A* **2000**, *62*, 063202.
(25) (a) Boldyrev, A. I.; Simons, J.; Schleyer, P. v. R. *J. Chem. Phys.* **1993**, *99*, 8793. (b) Boldyrev, A. I.; Gonzales, N.; Simons, J. *J. Phys. Chem.* **1994**, *98*, 9931.
(26) Nemukhin, A. V.; Almlof, J.; Heiberg, A. *Chem. Phys. Lett.* **1980**, *76*, 601.
(27) Tai, T. B.; Nhat, P. V.; Nguyen, M. T. *Phys. Chem. Chem. Phys.* **2010**, *12*, 11477.
(28) Kuma, V. *Phys. Rev. B* **1999**, *60*, 2916.
(29) Guo, X. Q.; Podloucky, R.; Freeman, A. J. *Phys. Rev. B* **1990**, *42*, 10912.
(30) Chacko, S.; Kanhere, D. G. *Phys. Rev. A* **2004**, *70*, 023204.
(31) Akola, J.; Manninen, M. *Phys. Rev. B* **2002**, *65*, 245424.
(32) Cheng, H. P.; Barnett, R. N.; Landman, U. *Phys. Rev. B* **1993**, *48*, 1820.
(33) Lee, M. S.; Gowtham, S.; He, H.; Lau, K. C.; Pan, L.; Kanhere, D. G. *Phys. Rev. B* **2006**, *74*, 245412.
(34) Lievens, P.; Thoen, P.; Bouckaert, S.; Bouwen, W.; Vanhoutte, W.; Weidele, H.; Silverans, R. E.; Vazquez, A. N.; Schleyer, P. v. R. *Eur. Phys. J. D* **1999**, *9*, 289.
(35) Lievens, P.; Thoen, P.; Bouckaert, S.; Bouwen, W.; Vanhoutte, F.; Weidele, H.; Silverans, R. E. *Chem. Phys. Lett.* **1999**, *302*, 571.
(36) Ivanic, J.; Marsden, C. J. *J. Am. Chem. Soc.* **1993**, *115*, 7503.
(37) Kudo, H. *Nature* **1992**, *355*, 432.
(38) Schleyer, P. v. R.; Wurthwein, E. U.; Kaufman, E.; Lark, T.; Pople, J. A. *J. Am. Chem. Soc.* **1983**, *105*, 5930.
(39) Joshi, K.; Kanhere, D. G. *Phys. Rev. A* **2002**, *65*, 043203.
(40) Shetty, S.; Pal, S.; Kanhere, D. G. *J. Chem. Phys.* **2003**, *118*, 7288.
(41) Joshi, K.; Kanhere, D. G. *J. Chem. Phys.* **2003**, *119*, 12301.
(42) Gopakumar, G.; Lievens, P.; Nguyen, M. T. *J. Phys. Chem.* **2007**, *111*, 4353.
(43) Ngan, V. T.; Haeck, J. H.; Le, H. T.; Gopakumar, G.; Lievens, P.; Nguyen, M. T. *J. Phys. Chem. A* **2009**, *113*, 9080.
(44) Lievens, P.; Thoen, P.; Bouckaert, S.; Bouwen, W.; Vanhoutte, W.; Weidele, H.; Silverans, R. E.; Vazquez, A. N.; Schleyer, P. v. R. J. *Chem. Phys.* **1999**, *110*, 10316.
(45) Meden, A.; Mavri, J.; Bele, M.; Pejovnik, S. *J. Phys. Chem.* **1995**, *99*, 4252.
(46) (a) Li, Y.; Wu, D.; Li, Z. R.; Sun, C. C. *J. Comput. Chem.* **2007**, *28*, 1677. (b) Li, Y.; Liu, Y. J.; Wu, D.; Li, Z. R. *Phys. Chem. Chem. Phys.* **2009**, *11*, 5703.
(47) (a) Nguyen, K. A.; Lammertsma, K. *J. Phys. Chem. A* **1998**, *102*, 1608. (b) Nguyen, K. A.; Srinivas, G. N.; Hamilton, T. P.; Lammertsma, K. *J. Phys. Chem. A* **1999**, *103*, 710.
(48) (a) Tai, T. B.; Nguyen, M. T. *Chem. Phys.* **2010**, *375*, 35. (b) Tai, T. B.; Nguyen, M. T. *Chem. Phys. Lett.* **2010**, *489*, 75.
(49) Knight, W. D.; Clemenger, K.; de Heer, W. A.; Saunders, W. A.; Chou, M. Y.; Cohen, M. L. *Phys. Rev. Lett.* **1984**, *52*, 2141.
(50) Frisch, M. J.; Trucks, G. W.; Schlegel, H. B.; Scuseria, G. E.; Robb, M. A.; Cheeseman, J. R.; Montgomery, J. A., Jr.; Vreven, T.; Kudin, K. N.; Burant, J. C.; Millam, J. M.; Iyengar, S. S.; Tomasi, J.; Barone, V.; Mennucci, B.; Cossi, M.; Scalmani, G.; Rega, N.; Petersson, G. A.; Nakatsuji, H.; Hada, M.; Ehara, M.; Toyota, K.; Fukuda, R.; Hasegawa, J.; Ishida, M.; Nakajima, T.; Honda, Y.; Kitao, O.; Nakai, H.; Klene, M.; Li, X.; Knox, J. E.; Hratchian, H. P.; Cross, J. B.; Bakken, V.; Adamo, C.; Jaramillo, J.; Gomperts, R.; Stratmann, R. E.; Yazyev, O.; Austin, A. J.; Cammi, R.; Pomelli, C.; Ochterski, J. W.; Ayala, P. Y.; Morokuma, K.; Voth, G. A.; Salvador, P.; Dannenberg, J. J.; Zakrzewski, V. G.; Dapprich, S.; Daniels, A. D.; Strain, M. C.; Farkas, O.; Malick, D. K.; Rabuck, A. D.; Raghavachari, K.; Foresman, J. B.; Ortiz, J. V.; Cui, Q.; Baboul, A. G.; Clifford, S.; Cioslowski, J.; Stefanov, B. B.; Liu, G.; Liashenko, A.; Piskorz, P.; Komaromi, I.; Martin, R. L.; Fox, D. J.; Keith, T.; Al-Laham, M. A.; Peng, C. Y.; Nanayakkara, A.; Challacombe, M.; Gill, P. M. W.; Johnson, B.; Chen, W.; Wong, M. W.; Gonzalez, C.; Pople, J. A. *Gaussian 03*, revision C.01; Gaussian, Inc.: Wallingford, CT, 2004.
(51) *MOLPRO*, version 2008.1, a package of ab initio programs. Werner, H.-J.; Knowles, P. J.; Lindh, R.; Manby, F. R.; Schütz, M.; Celani, P.; Korona, T.; Rauhut, G.; Amos, R. D.; Bernhardsson, A.; Berning, A.; Cooper, D. L.; Deegan, M. J. O.; Dobbyn, A. J.; Eckert, F.; Hampel C.; Hetzer, G.; Lloyd, A. W.; McNicholas, S. J.; Meyer W.; Mura, M. E.; Nicklass, A.; Palmieri, P.; Pitzer, R.; Schumann, U.; Stoll, H.; Stone, A. J.; Tarroni, R.; Thorsteinsson, T. See http://www.molpro.net.
(52) Parr, R. G.; Yang, W. *Density-Functional Theory of Atoms and Molecules*; Oxford University Press: Oxford, U.K., 1989.

(53) Becke, A. D. *J. Chem. Phys.* **1993**, *98*, 5648.
(54) Lee, C.; Yang, W.; Parr, R. G. *Phys. Rev. B* **1988**, *37*, 785.
(55) Kendall, R. A.; Dunning, T. H., Jr.; Harrison, R. J. *J. Chem. Phys.* **1992**, *96*, 6796.
(56) (a) Deegan, M. J. O.; Knowles, P. J. *Chem. Phys. Lett.* **1994**, *227*, 321. (b) Knowles, P. J.; Hampel, C.; Werner, H.-J. *J. Chem. Phys.* **1993**, *99*, 5219. (c) Rittby, M.; Bartlett, R. J. *J. Phys. Chem.* **1988**, *92*, 3033.
(57) (a) Curtiss, L. A.; Raghavachari, K.; Redfern, P. C.; Rassolov, V.; Pople, J. A. *J. Chem. Phys.* **1998**, *109*, 7764. (b) Baboul, A. G.; Curtiss, L. A.; Redfern, P. C. *J. Chem. Phys.* **1999**, *110*, 7650.
(58) Dunning, T. H., Jr. *J. Chem. Phys.* **1989**, *90*, 1007.
(59) Peterson, K. A.; Woon, D. E.; Dunning, T. H., Jr. *J. Chem. Phys.* **1994**, *100*, 7410.
(60) (a) Woon, D. E.; Dunning, T. H., Jr. *J. Chem. Phys.* **1995**, *103*, 4572. (b) Peterson, K. A.; Dunning, T. H., Jr. *J. Chem. Phys.* **2002**, *117*, 10548.
(61) (a) Douglas, M.; Kroll, N. M. *Ann. Phys.* **1974**, *82*, 89. (b) Hess, B. A. *Phys. Rev. A* **1985**, *32*, 756. (c) Hess, B. A. *Phys. Rev. A* **1986**, *33*, 3742.
(62) de Jong, W. A.; Harrison, R. J.; Dixon, D. A. *J. Chem. Phys.* **2001**, *114*, 48.
(63) Prascher, B. P.; Woon, D. E.; Peterson, K. A.; Dunning, T. H., Jr.; Wilson, A. K. *Theor. Chem. Acc.* **2010**, DOI: 10.1007/s00214-010-0764-0.
(64) Nguyen, M. T.; Matus, M. H.; Ngan, V. T.; Grant, D. J.; Dixon, D. A. *J. Phys. Chem. A* **2009**, *113*, 4895.
(65) Tai, T. B.; Grant, D. J.; Nguyen, M. T.; Dixon, D. A. *J. Phys. Chem. A* **2010**, *114*, 994.
(66) Tai, T. B.; Nguyen, M. T.; Dixon, D. A. *J. Phys. Chem. A* **2010**, *114*, 2893.
(67) Karton, A.; Martin, J. M. L. *J. Phys. Chem. A* **2007**, *111*, 5936.
(68) Chase, M. W., Jr. NIST-JANAF Thermochemical Tables, 4th ed.; *J. Phys. Chem. Ref. Data, Monograph 9*; American Institute of Physics: Woodbury, NY, 1998; Supplement 1.
(69) Feller, D.; Peterson, K. A.; Dixon, D. A. *J. Chem. Phys.* **2008**, *129*, 204105.
(70) Curtiss, L. A.; Raghavachari, K.; Redfern, P. C.; Pople, J. A. *J. Chem. Phys.* **1997**, *106*, 1063.
(71) Li, S. Ph.D. Thesis, University of Kentucky, 2004.
(72) Reed, A. E.; Curtiss, L. A.; Weinhold, F. *Chem. Rev.* **1988**, *88*, 899.
(73) Perdew, J. P.; Chevary, J. A.; Vosko, S. H.; Jackson, K. A.; Pederson, M. R.; Singh, D. J.; Fiolhais, C. *Phys. Rev. B* **1992**, *46*, 6671.
(74) Clark, T.; Chandrasekhar, J.; Spitznagel, G. W.; Schleyer, P. v. R. *J. Comput. Chem.* **1983**, *4*, 294.
(75) Becke, A.; Edgecombe, K. *J. Chem. Phys.* **1990**, *92*, 5397.
(76) (a) Silvi, B.; Savin, A. *Nature* **1994**, *371*, 683. (b) Savin, A.; Becke, A.; Flad, D.; Nesper, R.; Preuss, H.; Schnering, H. V. *Angew. Chem., Int. Ed.* **1991**, *30*, 409. (c) Savin, A.; Silvi, B.; Colonna, F. *Can. J. Chem.* **1996**, *74*, 1088.
(77) (a) Noury, S.; Krokidis, X.; Fuster, F.; Silvi, B. *TOPMOD Package*; Universite Pierre et Marie Curie: Paris, 1997. (b) Noury, S.; Krokidis, X.; Fuster, F.; Silvi, B. *Compt. Chem.* **1999**, *23*, 597.
(78) (a) Laaksonen, L. *J. Mol. Graph.* **1992**, *10*, 33. (b) Bergman, D. L.; Laaksonen, L.; Laaksonen, A. *J. Mol. Graph. Model* **1997**, *15*, 301.
(79) (a) Benichou, E.; Allouche, A. R.; Aubert-Frecon, M.; Antoine, R.; Broyer, M.; Dugourd, Ph.; Rayane, D. *Chem. Phys. Lett.* **1998**, *290*, 171. (b) Dugourd, Ph.; Rayane, D.; Labastie, P.; Vezin, B.; Chevaleyre, J.; Broyer, M. *Chem. Phys. Lett.* **1992**, *197*, 433.
(80) Lee, T. J.; Taylor, P. R. *Int. J. Quantum Chem.* **1989**, *S23*, 199.
(81) Huber, K. P.; Herzberg, G. *Molecular Spectra and Molecular Structure Constants of Diatomic Molecules*; van Nostrand-Reinhold: New York, 1979.
(82) Bernheim, R. A.; Gold, L. P.; Tipton, T. *J. Chem. Phys.* **1983**, *78*, 3653.
(83) McGeogh, M. W.; Schlier, R. E. *Chem. Phys. Lett.* **1983**, *99*, 347.
(84) Lide, D. R., Ed. *CRC Handbook of Chemistry and Physics*, 86th ed.; Taylor and Francis: Boca Raton, FL, 2005; pp 10−202.
(85) Lide, D. R., Ed.; *CRC Handbook of Chemistry and Physics*, 86th ed.; Taylor and Francis: Boca Raton, FL, 2005, pp 12−114.
(86) de Heer, W. A. *Rev. Mod. Phys.* **1993**, *65*, 611.
(87) Bouwen, W.; Vanhoutte, F.; Despa, F.; Bouckaert, S.; Neukermans, S.; Kuhn, L. T.; Weidele, H.; Lievens, P.; Silverans, R. E. *Chem. Phys. Lett.* **1999**, *314*, 227.
(88) Hoshino, K.; Watanabe, K.; Konishi, Y.; Taguwa, T; Nakajima, A.; Kaya, K. *Chem. Phys. Lett.* **1994**, *231*, 499.
(89) Kappes, M. M.; Radi, P.; Schar, M.; Schumacher, E. *Chem. Phys. Lett.* **1985**, *119*, 11.
(90) Yeretzian, C.; Rothlisberger, U.; Schumacher, E. *Chem. Phys. Lett.* **1995**, *237*, 334.
(91) Janssens, E.; Neukermans, S.; Lievens, P. *Curr. Opin. Solid. State Mater. Sci.* **2004**, *15*, 8.
(92) C. Yeretzian, C. *J. Phys. Chem.* **1995**, *99*, 123.
(93) Clemenger, K. *Phys. Rev. B.* **1985**, *32*, 1359. Nilsson, S. G. *K. Dan. Vidensk. Selsk, Mat. Fys. Medd.* **1955**, *29*, 16. Gustafson, C.; Lamm, I. L.; Nilsson, S. G. *Ark. Fys.* **1967**, *36*, 613.